The Plant Cell, Vol. 31: 1043–1062, May 2019, www.plantcell.org © 2019 ASPB.

Tomato MYB21 Acts in Ovules to Mediate Jasmonate-Regulated Fertility[OPEN]

Ramona Schubert,[a] Susanne Dobritzsch,[a] Cornelia Gruber,[a] Gerd Hause,[b] Benedikt Athmer,[a] Tom Schreiber,[a] Sylvestre Marillonnet,[a] Yoshihiro Okabe,[c] Hiroshi Ezura,[c] Ivan F. Acosta,[d] Danuse Tarkowska,[e] and Bettina Hause[a,1]

[a] Department of Cell and Metabolic Biology, Institute of Plant Biochemistry, 06120 Halle, Germany
[b] Martin Luther University Halle Wittenberg, Biocenter, Electron Microscopy, 06120 Halle, Germany
[c] Tsukuba Plant Innovation Research Center, University of Tsukuba, Tsukuba, Japan
[d] Max Planck Institute for Plant Breeding Research, 50829 Köln, Germany
[e] Laboratory of Growth Regulators, Palacky University and Institute of Experimental Botany, Czech Academy of Sciences, v.v.i., CZ-78371, Olomouc, Czech Republic

ORCID IDs: 0000-0003-0745-8295 (R.S.); 0000-0003-1823-4238 (S.D.); 0000-0002-5720-3904 (C.G.); 0000-0003-0242-3923 (G.H.); 0000-0002-0234-4398 (B.A.); 0000-0001-5457-178X (T.S.); 0000-0002-4263-797X (S.M.); 0000-0002-8741-9503 (Y.O.); 0000-0003-1443-2210 (H.E.); 0000-0001-7080-3384 (I.F.A.); 0000-0003-1478-1904 (D.T.); 0000-0001-9697-4990 (B.H.)

The function of the plant hormone jasmonic acid (JA) in the development of tomato (*Solanum lycopersicum*) flowers was analyzed with a mutant defective in JA perception (*jasmonate-insensitive1-1*, *jai1-1*). In contrast with Arabidopsis (*Arabidopsis thaliana*) JA-insensitive plants, which are male sterile, the tomato *jai1-1* mutant is female sterile, with major defects in female development. To identify putative JA-dependent regulatory components, we performed transcriptomics on ovules from flowers at three developmental stages from wild type and *jai1-1* mutants. One of the strongly downregulated genes in *jai1-1* encodes the MYB transcription factor SlMYB21. Its Arabidopsis ortholog plays a crucial role in JA-regulated stamen development. SlMYB21 was shown here to exhibit transcription factor activity in yeast, to interact with SlJAZ9 in yeast and in planta, and to complement Arabidopsis *myb21-5*. To analyze SlMYB21 function, we generated clustered regularly interspaced short palindromic repeats(CRISPR)/CRISPR associated protein 9 (Cas9) mutants and identified a mutant by Targeting Induced Local Lesions in Genomes (TILLING). These mutants showed female sterility, corroborating a function of MYB21 in tomato ovule development. Transcriptomics analysis of wild type, *jai1-1*, and *myb21-2* carpels revealed processes that might be controlled by SlMYB21. The data suggest positive regulation of JA biosynthesis by SlMYB21, but negative regulation of auxin and gibberellins. The results demonstrate that SlMYB21 mediates at least partially the action of JA and might control the flower-to-fruit transition.

INTRODUCTION

In seed plants, successful reproduction involves coordinated flower organ development followed by fertilization and fruit development. During flower development, organ specification, growth, and patterning are tightly controlled. The female reproductive organ, the gynoecium, goes through a complex growth and patterning process, after which it ceases growth until fertilization occurs (Johri et al., 1992). Following successful fertilization, seeds start to develop within the ovary, the lower part of the gynoecium, and the ovary resumes growth and develops into a fruit (Gillaspy et al., 1993; Larsson et al., 2014). Seeds themselves, however, originate from ovules, which in turn emerge from the placental tissue as finger-like primordia (Smyth et al., 1990; Modrusan et al., 1994). Ovule structure is largely conserved, and three different regions can be distinguished along the proximal-distal axis: (1) the nucellus, which encloses the megaspore/megagametophyte lineage; (2) the chalaza, which initiates the inner and outer integuments that grow around the nucellus; and (3) the funiculus, which attaches the ovule to the placenta and provides a physical and vascular connection to it (Schneitz et al., 1995). In tomato (*Solanum lycopersicum*), ovules are anatropous, unitegmic, and tenuinucellar, the latter meaning that no hypodermal cell layer is present between the meiocyte and nucellus apex (Brukhin et al., 2003; Endress, 2011). In these so-called thin ovules, often an endothelium is formed on the inside of the integument, and the endothelium appears to supply the embryo sac with nutrients (Kapil and Tiwari, 1978; Endress, 2010, 2011). After fertilization, seed development is initiated leading to the formation of embryo and endosperm (Drews and Yadegari, 2002). The maternal tissue of the ovule also undergoes drastic changes, such as a rapid phase of cell division and expansion in the integuments (Haughn and Chaudhury, 2005). In several plant species, the proximal region of the nucellus undergoes programmed cell death (PCD) and partially or totally disappears (Lu and Magnani, 2018).

Gynoecium and ovule patterning, growth, and maturation are tightly controlled to achieve successful reproduction. Several plant hormones, as well as their crosstalk, are involved in the regulation of these processes (Marsch-Martínez and de Folter, 2016). The plant hormones auxin and gibberellins (GAs) are

[1] Address correspondence to Bettina.Hause@ipb-halle.de.
The author responsible for distribution of materials integral to the findings presented in this article in accordance with the policy described in the Instructions for Authors (www.plantcell.org) is: Bettina Hause (Bettina.Hause@ipb-halle.de).
[OPEN]Articles can be viewed without a subscription.
www.plantcell.org/cgi/doi/10.1105/tpc.18.00978

IN A NUTSHELL

Background: The survival of most plant species depends on proper flower development, successful fertilization, fruit and seed set to obtain the next generation. These processes demand specific co-ordination between the different flower parts, which is partly regulated by plant hormones like jasmonate (JA), auxin and gibberellins (GA). JA plays an important role since mutants unable to detect the hormone (insensitive) are sterile. There are, however, differences between plant species referring to the strongest defects in male (stamen) or female (carpel) flower parts: The JA-insensitive mutant of the model plant *Arabidopsis thaliana* (mouse-ear cress) is strongly impaired in stamen development, where among others the transcription factor MYB21 plays a regulatory role. In contrast, the JA-insensitive tomato mutant is defective in carpel development and does not produce seeds.

Question: Although much is known about the JA-mediated role of MYB21 in stamen development of Arabidopsis, differences in the JA function in flower development between plant species are hardly understood and should be investigated here using tomato as a model crop plant.

Findings: We found that MYB21 is a key regulator in tomato flower development. In contrast to Arabidopsis, the main function is the regulation of the timing of the different flower parts with a special emphasis on carpel development. *myb21* mutants showed defects in flower opening and do not set seeds. Comparing the total gene expression in carpels of the JA-insensitive mutant, *myb21* and wild type flowers, we revealed a JA-dependent function of MYB21 in regulating expression of genes related to cell expansion and division as well as auxin signalling and GA-biosynthesis. Tomato MYB21 also regulated JA biosynthesis in a positive way. We concluded that MYB21 is involved into the regulation of JA, auxin and GA-homeostasis within the carpel to couple fertilization and fruit initiation processes.

Next steps: Follow-up work needs to be done in specifying the interplay between JA and other hormones in tomato flower development. Other open questions regard the genes, which are regulated by MYB21, and the interaction of MYB21 with other transcription factors.

important for gynoecium and fruit development (Larsson et al., 2014; Pattison et al., 2014; Goldental-Cohen et al., 2017; Moubayidin and Østergaard, 2017). Another group of plant hormones involved in flower development are jasmonates (JAs) including jasmonic acid (JA) and its derivatives. These lipid-derived compounds are ubiquitously occurring plant signaling compounds that act in the response to biotic and abiotic stress, and in development (Wasternack and Hause, 2013). JA synthesized from α-linolenic acid released from plastid membranes is enzymatically converted into (+)-7-*iso*-jasmonoyl isoleucine (JA-Ile; Wasternack and Song, 2017), which represents the most biologically active form of JAs by mediating binding of the coreceptor proteins CORONATINE INSENSITIVE1 (COI1) and JASMONATE ZIM DOMAIN (JAZ; Chini et al., 2007; Thines et al., 2007; Fonseca et al., 2009). The JA response involves the activity of transcription factors (TFs), such as basic helix-loop-helix (bHLH) TFs like MYC2, which are repressed by JAZ proteins in the resting state of a plant. Rise in JA-Ile leads to the interaction of COI1 and JAZ, thereby mediating the proteasomal degradation of JAZ and freeing TFs such as MYC2 from repression (Wasternack and Hause, 2013).

Characterization of JA-insensitive or -deficient mutants provided strong evidence for the involvement of JA in flower development. Arabidopsis (*Arabidopsis thaliana*) JA-insensitive plants mutated in the JA-coreceptor COI1 (*coi1*) or JA-deficient plants mutated in JA-biosynthetic genes (e.g., *allene oxide* synthase, *OPDA reductase3*) are male sterile (Browse, 2009a). All of these mutants do not produce seeds due to an identical male-sterile phenotype with nonelongating stamen filaments, nondehiscent anthers, and nongerminating pollen (Browse, 2009b, 2009a). Several TFs have been shown to regulate JA-mediated stamen development, such as the R2R3-MYB-TFs MYB21, MYB24, and MYB108 (Mandaokar et al., 2006). Mutants affected in these TFs mirror to some extent the phenotype of JA-insensitive plants, exhibiting reduced male fertility that is associated with nonelongated filaments, delayed anther dehiscence, reduced pollen viability, and decreased fecundity relative to wild type (Mandaokar and Browse, 2009; Song et al., 2011). Interestingly, overexpression of *AtMYB21* in *coi1* or of *AtMYB24* in *OPDA reductase3* could partially rescue male fertility, suggesting a central role for both TFs in Arabidopsis stamen and pollen development (Song et al., 2011; Huang et al., 2017). AtMYB21 and AtMYB24 are targets of JAZ repressors (Song et al., 2011; Huang et al., 2017), but interact additionally with bHLH TFs of the IIIe clade, such as MYC2, MYC3, MYC4, and MYC5, to form a bHLH-MYB transcription complex that cooperatively regulates stamen development (Qi et al., 2015).

A JA-insensitive mutant in tomato (cv Micro-Tom), called *jasmonic acid-insensitive1-1* (*jai1-1*), exhibits a 6.2-kb deletion in the tomato ortholog of *AtCOI1* (Li et al., 2004). This mutant is, however, female sterile and does not produce seeds upon pollination with wild type or *jai1-1* pollen, although fruit set and fruit development appear similar to wild-type plants (Li et al., 2004).The *jai1-1* plants also exhibit some defects in the male reproductive function, such as a reduction in pollen viability and germination. The fertilization capability of pollen is, however, not affected (Li et al., 2004). Comparative transcript profiling of wild-type and *jai1-1* stamens showed that genes encoding enzymes involved in the biosynthesis of ethylene (ET) and ET-related TFs as well as ET-response genes are expressed earlier during stamen development of *jai1-1* in comparison with that of wild type (Dobritzsch et al., 2015). This premature ET function might cause enhanced dehiscence of the *jai1-1* stamen in the open flower and misregulated pollen maturation and release. An additional phenotypic feature of *jai1-1* mutant flowers is a swollen gynoecium, which in combination with the senescent stamen leads to a

protrusion of the stigma from the anther cone of mature flowers (Li et al., 2004).

The female sterility of *jai1-1* is in agreement with data showing that JA biosynthesis might occur predominantly in ovules, where one of the JA-biosynthetic enzymes, ALLENE OXID CYCLASE, is preferentially located (Hause et al., 2000). Moreover, JA and JA-Ile accumulate mainly in the carpel of flower buds highly exceeding the levels detected in nonstressed leaves (Hause et al., 2000). This organ-specific accumulation of JA/JA-Ile may result in organ-specific regulation of gene expression. Indeed, a number of JA-induced genes are specifically expressed within ovules (Hause et al., 2000), but their regulation by JA in gametophytic organs has not yet been proven. To address this question, we used wild type and *jai1-1* flower buds at different developmental stages and performed an integrated approach by immunological detection of JA/JA-Ile and comparative transcript profiling of ovules. The obtained data and further histological analyses showed that the nucellus of *jai1-1* flowers undergoes a premature PCD and that SlMYB21, an ortholog of AtMYB21, might be involved in its regulation. To test these results, three *Slmyb21* mutants were identified by TILLING or generated by clustered regularly interspaced short palindromic repeats (CRISPR)/CRISPR associated protein 9 (Cas9) genome editing. Comparing transcript and hormone profiles of carpels from *Slmyb21-2* and *jai1-1* suggested that SlMYB21 regulates JA biosynthesis positively in female organs of tomato. In addition, SlMYB21 may mediate JA function in carpel and ovule development via regulation of auxin and GAs biosynthesis and signaling.

RESULTS

Wild-type Carpels of Large Flower Buds Contain Highest JA/JA-Ile Levels

Previous work revealed that the timing of flower development in wild-type and *jai1-1* plants is very similar, showing the same developmental stages ranging from small flower buds up to open flowers (Dobritzsch et al., 2015). Six stages were classified using parameters such as bud size, sepal opening, and petal color. The youngest stage (1) represented a small bud completely enclosed by sepals; the mid–bud-stage (3) was characterized by slightly opened sepals and greenish-white petals; and the oldest stage (6) represented the open flower showing bright yellow petals. Open flowers of both genotypes differ by prominent phenotypic features of *jai1-1*, such as the protrusion of the stigma out of the stamen cone and the senescing tip of the stamen cone (Li et al., 2004; Dobritzsch et al., 2015). Additionally, detailed inspection of the carpels revealed that in *jai1-1* they appear larger than in wild type (Figure 1A) reaching up to 100% higher fresh weight and 50% higher dry weight than in wild type (Supplemental Figures 1A and 1B). The enhanced growth of *jai1-1* carpels might be one reason for the protrusion of the stigma from the stamen cone.

Previous data suggested the synthesis of JAs specifically in ovules due to the preferential occurrence of the biosynthetic enzyme ALLENE OXID CYCLASE in these organs (Hause et al., 2000). Therefore, levels of JA and JA-Ile were determined in wild-type and *jai1-1* carpels collected at each developmental stage (Figure 1B). The levels of both JA and JA-Ile exhibited a significant maximum in wild-type carpels at stage 3, but dropped down below the detection limit at stages 4 and 5, respectively (Figure 1B). Most importantly, the levels of both compounds were almost below the detection limit in *jai1-1* carpels at all developmental stages.

To get insights into the possible occurrence of JAs in ovules, we used immunohistochemistry with a specific antibody against JA/JA-Ile and our established protocol (Mielke et al., 2011), JAs were visualized in cross sections of wild-type carpels of developmental stages 1, 3, and 6 covering low, high, and nondetectable levels of JA/JA-Ile, respectively. Carpels of *jai1-1* flower buds at stage 3 lacking JAs served as negative control. The strongest label indicative for the occurrence of JA/JA-Ile occurred in wild-type carpels of stage 3, whereas carpels of wild-type stage 6 and *jai1-1* did not show green fluorescence above the background (Figure 1C). Furthermore, JA and JA-Ile were detectable in ovules of wild-type flower buds at stage 1 and even stronger at stage 3, but not in ovules of *jai1-1* flower buds (Figure 1D), suggesting that JAs may function in wild-type ovules of stage 3.

Jasmonate-Insensitivity Alters the Transcriptome in Ovules

To analyze the activity of JAs in transcriptional responses during ovule development, transcript profiling was conducted for wild-type and *jai1-1* ovules of developmental stages with the maximal difference in JA/JA-Ile contents in wild type, i.e., stages 1, 3, and 6. RNA isolated from dissected ovules at these stages was used for hybridization of Agilent Tomato Arrays. The comparison between ovules of wild type and *jai1-1* in each of the three analyzed stages revealed 383 differentially expressed genes (DEG) in ovules of both genotypes (Figure 2A; Supplemental Data Set 1). Almost two third of the identified genes showed a stage-specific, differential expression, whereas one third of genes appeared to be differentially expressed in two or three developmental stages. Among the stage-specific DEG, the number of DEG correlated with JA/JA-Ile levels: The lowest number of DEG was detected in stage 1 showing low JA/JA-Ile levels in wild type and no obvious phenotypical differences between wild type and *jai1-1* (Figures 1A and 1B), whereas the highest number of DEGs occurred in stage 3. The identified DEG could be assigned to 22 functional classes (Figure 2B; Supplemental Data Set 1). The highest number of DEG occurred in the class “transcription factors and regulators” (36) followed by “secondary metabolism” (28), “defense” (26), and “proteinase inhibitors” (19).

Most of the DEG occurring in flower stages 1, 1+3, and 1+3+6 of the Venn diagram showed lower or almost no detectable expression in *jai1-1* (blue-labeled numbers in Figure 2B), whereas DEG occurring in developmental stages 3+6 and 6 exhibited higher expression levels in *jai1-1* than in wild-type ovules (brown-labeled numbers in Figure 2B). Most of the genes showing a strong downregulation in *jai1-1* include well-characterized JA-induced genes, such as *proteinase inhibitor II* and *cathepsin D inhibitor*, which are involved in JA-mediated defense (Wasternack and Hause, 2013). Other strictly JA-regulated genes are the well-described genes encoding JAZ proteins (Thines et al., 2007), such as *JAZ2* and *JAZ6*, and TFs, such as *SlMYB21* and *SlMYB14*. Transcript levels of most of these genes exhibited a maximum at

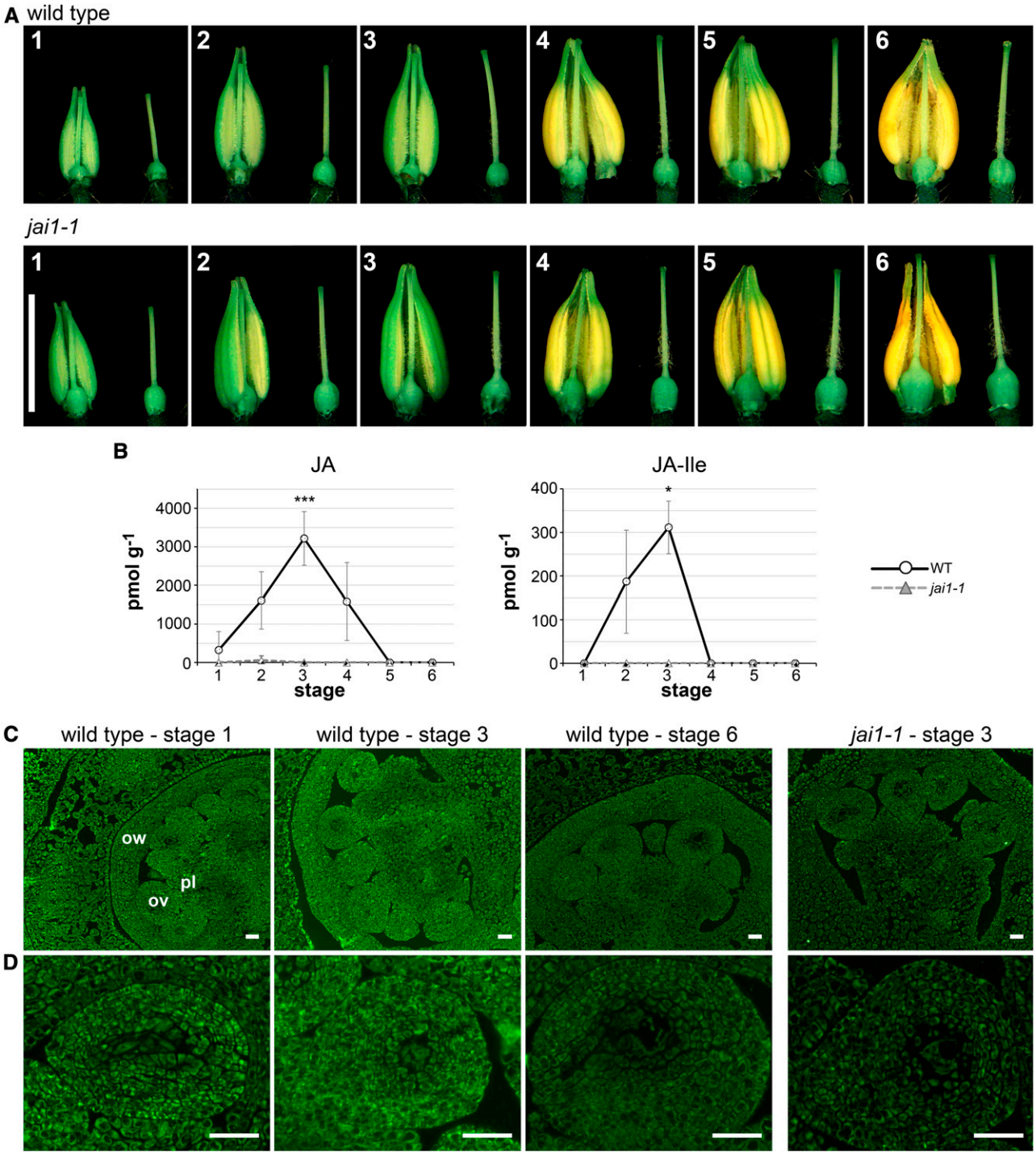

Figure 1. Classification of Stages and Levels of Jasmonates in Developing Carpels of Wild Type (WT) and *jai1-1*.

(A) Developmental stages of opened stamen cones and dissected carpels of wild type and *jai1-1* showing the six developmental stages as defined by Dobritzsch et al. (2015). In the picture down left, bar = 5 mm for all photographs.

(B) JA and JA-Ile levels in developing carpels. Carpels of the respective stage were extracted, and contents of JA and JA-Ile were determined. Mean values ±SD are shown ($n \geq 3$ independent pools of carpels). Data of the same developmental stage were compared between wild type and *jai1-1* by Student's *t* test (* $P \leq 0.05$, ** $P \leq 0.01$, *** $P \leq 0.001$).

(C) and (D) Immunocytochemical detection of JA/JA-Ile in ovaries **(C)** and ovules **(D)** of wild type and *jai1-1*. Carpels of wild type flowers at stages 1, 3, and 6 and of *jai1-1* at stage 3 were harvested, fixed with 1-ethyl-3-(3-dimethyl aminopropyl)-carbodiimide hydrochloride (EDC), and processed for

stage 3 of wild-type ovules correlating with the maximum JA/JA-Ile levels and are nearly undetectable in *jai1-1* ovules as validated by quantitative RT-PCR with RNA from ovules of an independent experiment (Figure 2C). This indicates a positive regulatory role of JAs during ovule development including an improved defense status as previously suggested (Hause et al., 2000).

Several DEG occurring specifically in stages 3 and 6 exhibited increased accumulation in ovules of *jai1-1* in comparison with wild type (Figures 2B and 2D). This suggests a negative regulatory role of JAs in late stages of ovule development. Mainly in stage 6 (open flower), several genes belonging to proteases (e.g., *METACASPASE9* and *SUBTILASES*), nucleases (e.g., *ENDONUCLEASE*), and cell wall modifying enzymes (e.g., *ENDOGLUCANASE* and *β-GLUCOSIDASE*) are strongly upregulated in *jai1-1* ovules (Figure 2D). It is possible that the enzymes encoded by these genes might mediate morphological changes in *jai1-1* ovules, since proteases and nucleases have been implicated in nucellus degeneration by PCD (Lu and Magnani, 2018). Therefore, ovule morphology was analyzed in carpel cross sections (Figure 3). Ovules of early developmental stages (stage 1–3) were almost undistinguishable between wild type and *jai1-1* (Supplemental Figure 2). At stages 4 and 5, however, the innermost cell layer of the nucellus of *jai1-1* ovules showed a thickening of the cell walls, which was not visible in wild-type ovules (Figure 3A; Supplemental Figure 2). Indeed, *jai1-1* ovules at stage 5 exhibited increased amounts of callose around the inner cells of the nucellus as visualized by immunostaining with an antibody against callose (Figure 3B), whereas in wild-type ovules callose was visible at plasmodesmata only (see inset in Figure 3B, wild type). Another obvious morphological difference was the occurrence of vacuoles in cells of the innermost cell layer of *jai1-1* nucellus at stage 6 (Figure 3A). Both, increased callose deposition and cell vacuolation, might be features of PCD. Testing this by a terminal deoxynucleotidyl transferase dUTP nick end labeling (TUNEL) assay showed much higher TUNEL-positive cells in *jai1-1* ovules, particularly in the innermost cells of the nucellus (Figure 3C). The abnormal morphology and the PCD occurring in these cells support the hypothesis drawn from transcript data that a premature elimination of the nucellus might occur in *jai1-1* ovules. Nucellus elimination is typically dependent on fertilization (Xu et al., 2016). The lack of JA function in *jai1-1* seems to uncouple fertilization and nucellus degeneration.

Jasmonate-Regulated *SlMYB21* Encodes a Flower-Specific Transcription Factor

Several genes encoding putative MYB-TFs were highly expressed in wild-type ovules, but were nearly undetectable in ovules of *jai1-1* (Figure 2) including SlMYB21 (*Solyc02g067760*). The putative SlMYB21 protein shows 64% sequence identity with Arabidopsis MYB21 (AtMYB21), which is known as an important regulator of JA-mediated stamen development (Mandaokar and Browse, 2009; Song et al., 2011). *SlMYB21* seems to be predominantly expressed in flower buds and open flowers as revealed by in silico analyses using tomato eFP browser (http://bar.utoronto.ca/) and the TomExpress database (Zouine et al., 2017; Supplemental Figures 3A and 3B). In dissected wild-type carpels, *SlMYB21* transcripts accumulated with a transient maximum in flowers at stages 4 and 5 (Supplemental Figure 3C). To test, whether the protein encoded by *Solyc02g067760* acts indeed as TF, we investigated its localization and transcriptional activity. Transient expression of a green fluorescent protein (*GFP*):*SlMYB21* fusion in *Nicotiana benthamiana* leaves showed that the protein is located predominantly in the nucleus (Figure 4A). Moreover, SlMYB21 displayed transcription-inducing activity in yeast as its fusion to the GAL4 binding domain (BD) alone resulted in transcriptional activity (Figure 4B). The previously detected interaction of AtMYB21 with several JAZ proteins (Song et al., 2011; Huang et al., 2017) prompted us to investigate putative interaction of SlMYB21 with the tomato JAZ proteins. All 12 known JAZ proteins from tomato were tested for their interaction with SlMYB21 in a yeast-two-hybrid (Y2H) assay (Figure 4C). Surprisingly, SlMYB21 interacted only with SlJAZ9. Analyzing all combinations by bimolecular fluorescence complementation (BiFC), positive signals were found for JAZ9 and JAZ8 (Figure 4D). According to eFP browser, *SlJAZ9* is mainly expressed in unopened flower buds, whereas *SlJAZ8* is exclusively expressed in roots (not shown). Consequently, an interaction between SlMYB21 and JAZ8 may not be relevant in flowers. All other JAZ proteins did not show an interaction with SlMYB21 in the BiFC assays (not shown). The interaction of SlMYB21 with JAZ9 was further validated by the split transcription activator-like effector(TALE) system (Schreiber et al., 2019). The fusion of SlMYB21 to the activation domain (AD) and of JAZ9 to the BD of TALE did not result in induction of the reporter construct (Supplemental Figure 4). However, fusion of $TALE^{BD}$ and $TALE^{AD}$ to JAZ9 and SlMYB21, respectively, resulted in a TALE reconstitution leading to significantly increased β-glucuronidase (GUS) activity (Figure 4E). Similar to yeast, SlMYB21 fused to $TALE^{BD}$ displayed transcriptional activity on its own, which was increased by coexpression of JAZ9-$TALE^{AD}$. Removing the AD of SlMYB21 almost abolished the activity of the fusion construct, but coexpression of JAZ9-$TALE^{AD}$ increased the activity ~4-fold. Thus, SlMYB21 exhibits transcriptional activity, and its interaction with one of the JAZ proteins of tomato suggests that this TF, like AtMYB21 (Song et al., 2011), might act at a hierarchical position in the JA signaling pathway (i.e., downstream of the COI1-JAZ coreceptor complex).

The high similarity of SlMYB21 and AtMYB21 prompted us to test whether SlMYB21 would be able to rescue the Arabidopsis

Figure 1. (continued).

immunolabeling as described by Mielke et al. (2011). The occurrence of JA is indicated by the green fluorescence. Note the strongest label in wild-type carpels at stage 3, whereas fluorescence signal is faint in carpels and ovules of *jai1-1*. Bars = 50 μm for all micrographs. Abbreviations: ov, ovule; pl, placenta; ow, ovary wall.

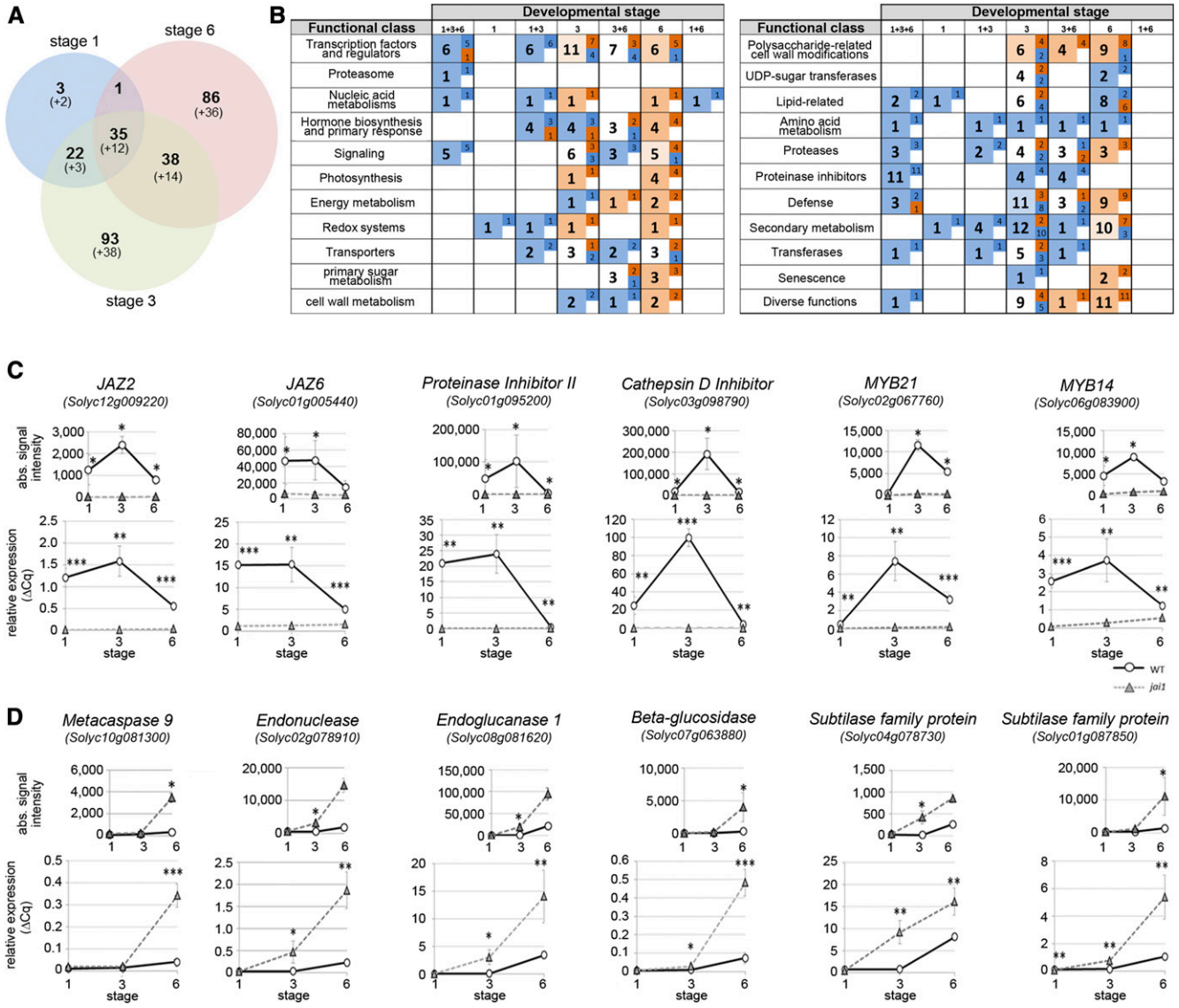

Figure 2. Comparative Analysis of Transcript Accumulation in Dissected Ovules of Wild Type (WT) and *jai1-1*.

Total RNA isolated from three developmental stages of ovules of wild type and *jai1-1* was subjected to transcript profiling using the Agilent-Tomato 44K-full genome chip.

(A) Venn diagram showing the number of significantly regulated genes ($P \leq 0.01$, $n = 3$ independent pools of dissected ovules). Numbers in parentheses are related to genes with unknown functions. Note that the highest number of differentially regulated genes was found in stage 3.

(B) Classification of differentially expressed genes according to functional classes. The bold numbers indicate how many genes in total were differentially regulated in the respective developmental stage, whereas the regular numbers show how many of them exhibited decreased (dark blue) or increased transcript levels in *jai1-1* (dark brown). Light blue and light brown colors mark the overall tendency of differential transcript accumulation in each developmental stage/functional class (blue higher in wild type, brown higher in *jai1-1*).

(C) and (D) Relative transcript levels of genes positively **(C)** and negatively **(D)** regulated by JA. Note that transcripts of the typical JA-regulated genes shown in **(C)** are nearly not detectable in ovules of *jai1-1*. All transcript levels were determined by RT-qPCR and set in relation to *SlTIP41* (rel. expression). The inset in each diagram visualizes the absolute signal intensity (abs. signal int.) obtained from microarray analysis. Mean values ±SD are shown ($n = 3$). Data of the same developmental stage were compared between wild type and *jai1-1* by Student's *t* test (*$P \leq 0.05$, **$P \leq 0.01$, ***$P \leq 0.001$). ▪○▪ wild type, —△— *jai1-1*

mutant *myb21-5*. Flowers of *Atmyb21-5* are characterized by short petals, short stamen filaments, and delayed flower opening and anther dehiscence (Reeves et al., 2012). Complementation of *Atmyb21-5* by expressing *AtMYB21* under the control of its endogenous promoter (*pAtMYB21*) resulted, however, only in a partial rescue that was characterized by an intermediate phenotype with increased filament length, dehiscent anthers, and opened flowers (Figure 4F). Out of eight independent lines, three developed seed-containing siliques. A similar partial and variable rescue of *myb21-5* using a *35S:GFP-AtMYB21*

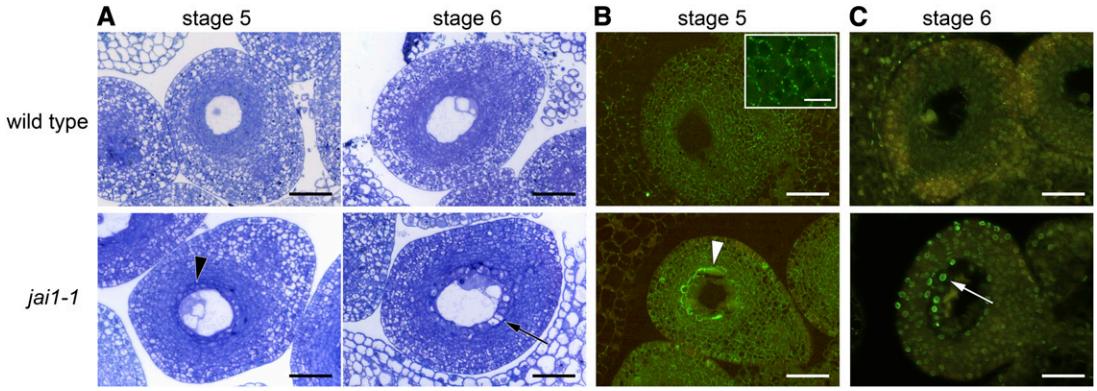

Figure 3. Ovules of *jai1-1* Show Altered Morphology and Exhibit Enhanced Callose Accumulation and PCD in the Nucellus.

(A) Semi-thin cross sections of ovules stained with toluidine blue. The developmental stages are indicated by numbers. Note the thickened cell walls in stage 5 (arrow head) and vacuolated cells of the inner layer of nucellus in stage 6 (arrow) of *jai1-1*.

(B) Immunolabeling of callose in ovules of stage 5. Callose visualized by green fluorescence is detectable in small spots between all cells of wild type ovules pointing to plasmodesmata (see inset), but surrounds additionally the innermost cell layer of the nucellus of *jai1-1* ovules.

(C) Cross sections of ovules at stage 6 were analyzed by the TUNEL assay. The wild type tissues only showed few TUNEL-positive signals. In contrast, a higher number of TUNEL-positive signals appeared in the innermost cell layer of the nucellus of the *jai1-1* mutant. Positive and negative controls showed labeling of all and no nuclei, respectively (Supplemental Figure 2B). Bars = 50 μm in all micrographs, except the inset, where it = 10 μm.

construct has been previously observed (Reeves et al., 2012). Expression of tomato *MYB21* under control of *pAtMYB21* rescued *Atmyb21-5* to a similar degree than Arabidopsis *MYB21* (Figure 4F). Out of six independent lines, two were able to develop seed-containing siliques (Figure 4F). These data support the conclusion that SlMYB21 is a functional equivalent of AtMYB21.

SlMYB21 Promotes Fertility, Ovule Development, and Jasmonate Biosynthesis

For functional analysis of SlMYB21, a *Slmyb21* mutant was selected by a TILLING approach (Okabe et al., 2011). Screening of the TILLING population resulted in four different mutants exhibiting a single base exchange within the two first exons of the SlMYB21 encoding gene (TOMJPE7564, TOMJPE7979, TOMJPE8245, and TOMJPW0469). Three of them were not altered in any property of MYB21, but TOMJPW0469 (*Slmyb21-1)* showed the exchange of a highly conserved Leu to a Lys residue within the first MYB domain, possibly affecting its transcription-inducing activity and/or DNA binding capability (Supplemental Figure 5A). Homozygous *Slmyb21-1* mutant plants showed abnormal flower development with petals that did not fully open and hardly developed fruits (Supplemental Figure 5B). In addition, two independent mutants were obtained using the CRISPR/Cas9 gene editing system (Brooks et al., 2014) targeting the second exon of *SlMYB21*. Twenty-nine independent transformants were obtained expressing *Cas9* and showing mutations in *SlMYB21*, 25 of which did not develop seeds. Among the eleven *Cas9*-positive and seed-producing lines, two different heterozygous offspring led to homozygous plants in the T2 generation (Figure 5). One of them showed a deletion of one T (*Slmyb21-2*) and the other an insertion of one T (*Slmyb21-3*), both of which are predicted to cause a premature stop codon and formation of a truncated, nonfunctional SlMYB21 (Figure 5A). The flower phenotype of both mutants was very similar to that of *Slmyb21-1* and showed the same defects in flower morphology (Figure 5B). In contrast with *Slmyb21-1*, *Slmyb21-2* and *Slmyb21-3* plants developed fruits, which were all seedless. *Slmyb21-2* plants were, however, capable to develop few seeds after hand pollination performed before flower opening. Ovules of all three *Slmyb21* mutants showed a phenotype like *jai1-1* ovules and exhibited accumulation of callose and vacuolated cells in the inner cell layer of the nucellus, although not so severe as *jai1-1* ovules (Figure 5C; Supplemental Figures 5C and 5D). In addition, flower buds of *myb21-2* at stage 3 were significantly longer than wild-type buds and *myb21-2* carpels exhibited higher fresh weight than wild-type carpels similarly to carpels of *jai1-1* (Supplemental Figures 1 and 6).

AtMYB21 was described to decrease JA levels through a negative feedback loop on the expression of JA biosynthesis genes (Reeves et al., 2012; Huang et al., 2017). We therefore determined JA and JA-Ile levels in carpels of the tomato *myb21* mutants in comparison with wild type and *jai1-1* (Figure 5D). For these determinations, carpels of flower buds at stage 3 were used, since they showed the highest levels of JA and JA-Ile in wild type (Figure 1B). Surprisingly, carpels of all three *slmyb21* mutants exhibited diminished JA and JA-Ile levels in comparison with those of wild type (Figure 5D). This points to a putative positive regulatory function of SlMYB21 on JA biosynthesis, which is opposite to its function in Arabidopsis.

SlMYB21 Contributes to Jasmonate-Regulated Gene Expression in Carpels

The similar phenotype of *Slmyb21* mutants and *jai1-1* suggests that the JA-induced TF SlMYB21 might mediate at least some of the JA-regulated processes, which are important for female fertility. To explore the putative regulatory hierarchy, a transcript

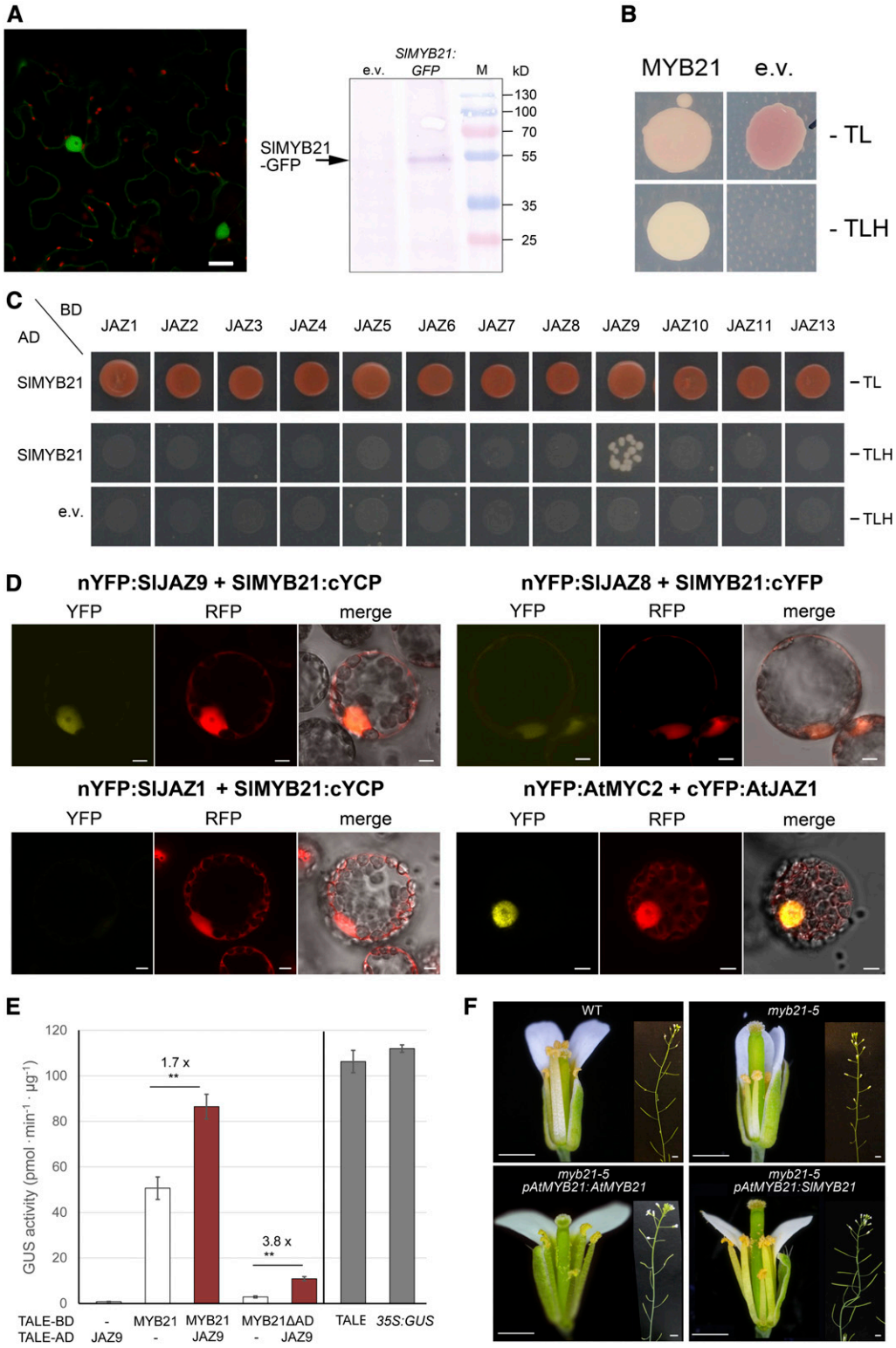

Figure 4. *SlMYB21* Encodes an Active Transcription Factor That Interacts With SlJAZ9 and Complements the Arabidopsis Mutant *myb21-5*.

(A) SlMYB21 is located in the nucleus as shown by transient expression of a *35S:gMYB21:GFP* construct in *N. benthamiana* leaves. The green fluorescence of the fusion protein is detectable in nuclei of the epidermal cells. Plastids are visible by their red autofluorescence. Protein gel blot performed with total

profiling by RNA sequencing (RNA-seq) was performed using dissected carpels at stage 3 from wild type, *jai1-1*, and *Slmyb21-2* (Figure 6). When comparing transcript levels of mutants with those from with wild type, in total 2016 DEG were found in both mutants (Supplemental Data Set 2). Among them, 1220 and 316 were differentially expressed exclusively in *jai1-1* and *Slmyb21-1*, respectively. Here, strictly JA-induced genes encoding defense proteins, such as PI-I, and encoding JA-signaling components, such as JAZ proteins and COI1, did not appear to be regulated by SlMYB21, since they were not found among the genes differentially regulated in *Slmyb21-2* (Figure 6B). In contrast, genes encoding stress-related proteins, such as thaumatin and LEA proteins, as well as several TFs seemed to be regulated independently of JA by SlMYB21, since they appear exclusively among the DEGs of *Slmyb21-2*. Most importantly, however, there were 237 and 226 DEG commonly up- and downregulated, respectively, in both mutants. This supports the hypothesis that at least a part of JA-regulated genes might be regulated by SlMYB21 (Figure 6A).

Gene Ontology analyses revealed that the DEGs occurring commonly in both mutants belong to various cellular processes (Supplemental Figure 7). Among them, the groups "auxin-activated signaling pathway" and "gibberellic acid mediated signaling pathway" showed several genes that were nearly not expressed in wild-type carpels, but significantly upregulated in carpels of both mutants (Figures 6C and 6D). The group of GA-related genes includes with ent-copalyl diphosphate synthase (*Solyc06g084240*), GA 20-oxidase-1, GA 20-oxidase-3, GA 3-β-hydroxylase, and GA 2-oxidase encoding genes, mainly GA-biosynthesis–related genes. Validation of RNA-seq-data by quantitative RT-PCR using RNA from carpels of an independent experiment showed that a selection of these genes indeed exhibits higher transcript levels in carpels of both mutants than in carpels of wild-type plants (Figure 6E; Supplemental Table 1). In addition, TFs, such as MYB12, a bHLH TF and an AP2-like TF, as well as pectin-related and fertilization-related genes, such as *expansin45*, two pectin esterases (*Solyc03g083770* and *Solyc11g019910*) and one pectin acetyl esterase (*Solyc08g014380*), were among the commonly upregulated genes. In contrast, several TF-encoding genes, like the homolog of Arabidopsis *BIGPETALp* bHLH-TF (*Solyc03g113560*; Varaud et al., 2011) and *S. lycopersicum fruit SANT/MYB-like1* (*SlFSM1*; Machemer et al., 2011), some auxin-related genes, and genes encoding proteins involved in cell-wall modification/cell organization, like two cellulose synthases (*Solyc08g082640* and *Solyc03g005450*), were positively regulated by JAs and SlMYB21, since they exhibit high transcript levels in wild type and low transcript levels in both mutants (Figure 6F; Supplemental Table 2). Among them, *SlMYB21* was drastically downregulated in carpels of both mutants. Moreover, the *SlMYB21* homolog *SlMYB24* is similarly downregulated suggesting the occurrence of a SlMYB21/SlMYB24 pair as described for Arabidopsis stamen development (Mandaokar et al., 2006).

Jasmonates and SlMYB21 Regulate GA Metabolism in Carpels

GAs play an important role in flower development, mainly in the developmental switch from flower to fruit after fertilization, since GA levels increase in the ovary upon pollination and exogenous application of GA to flowers induces parthenocarpy (Gorguet et al., 2005). This and the higher expression levels of GA biosynthesis genes in the mutants prompted us to determine levels of various gibberellin compounds in carpels of flower bud stage 3 from all three genotypes. We detected 15 different GAs including biosynthetic precursor, bioactive compounds, and inactive metabolites (Supplemental Table 3). A simplified biosynthetic pathway leading to the bioactive compounds GA_1, GA_3, GA_4, and GA_7 (Hedden and Phillips, 2000) from the precursors GA_{12} and GA_{53} is shown in Figure 7 along with their levels in carpels of wild type,

Figure 4. (continued).

protein extract from transformed leaves (empty vector and *35S:SlMYB21:GFP*) and an anti-GFP antibody shows the correct size of the fusion protein as indicated by the molecular weight marker **(M)**. Bar in the micrograph = 20 μm.

(B) Yeast assay used to detect the transcriptional activity of SlMYB21. Yeast cells transformed with *SlMYB21* fused to the GAL4 BD and the empty vector encoding the GAL4 AD were grown on synthetic defined (SD) medium without tryptophan and leucine (-TL) or SD medium without tryptophane, leucine and histidine (-TLH). Transformation with the empty vector (e.v.) only served as negative control.

(C) Y2H assays testing the interaction of SlMYB21 with SlJAZ proteins. Full-length CDS of all 12 SlJAZ proteins (JAZ1–JAZ11, JAZ13) were fused with the GAL4 BD and CDS of SlMYB21 was fused with the GAL4 AD. Transformed yeast cells were grown on SD/-TLH to determine protein–protein interactions. Positive yeast transformations are visualized by growth on SD/-TL. Omitting SlMYB21 by using the empty vector (e.v.) served as control and did not show yeast growth on SD/-TLH.

(D) BiFC assays performed to test the interaction of SlMYB21 with SlJAZ proteins. CDS of all 12 SlJAZ proteins (JAZ1–JAZ11, JAZ13) and of SlMYB21 were introduced in the 2in1 vectors (Grefen and Blatt, 2012), transformed into *N. benthamiana* protoplasts, and analyzed by confocal laser scanning microscopy. Interaction of SlMYB21 with SlJAZ9 and SlJAZ8 was detectable, whereas all other JAZ proteins did not show interaction as exemplified shown for SlJAZ1. Interaction of AtMYC2 with AtJAZ1 served as positive control. Bars = 5 μm.

(E) splitTALE assay showing the interaction of SlMYB21 with SlJAZ9 in planta. CDS of SlMYB21 with or without AD (C-terminal deletion of 25 aa) and SlJAZ9 were fused either to the TALE BD (N-terminal) or to AD (C-terminal), respectively, and expressed together with the reporter construct *4xSTAP1:GUS* in leaves of *N. benthamiana*. Transcriptional activity of full-length SlMYB21 fused to TALE BD is visible by a high GUS activity, which was enhanced by coexpression with SlJAZ9 fused to TALE-AD. Removal of AD of SlMYB21 resulted in lower basal activity, but was significantly increased by coexpression of SlJAZ9 fused to TALE-AD. Expression of complete TALE together with the reporter as well as *35S:GUS* served as positive controls. Mean values ±SE are shown ($n = 3$ different plants). Data were compared between expression of *SlMYB21* alone and together with *SlJAZ9* by Student's *t* test (**$P \leq 0.01$).

(F) Comparison of Arabidopsis flowers from different genotypes as indicated. As shown by one example out of eight and five independent lines, expression of *pAtMYB21:AtMYB21* results in partial rescue of the phenotype leading to seed set, which is also visible by expression of *pAtMYB21:SlMYB21*. Bars = 1 mm for flowers and 1 cm for shoots. WT, wild type.

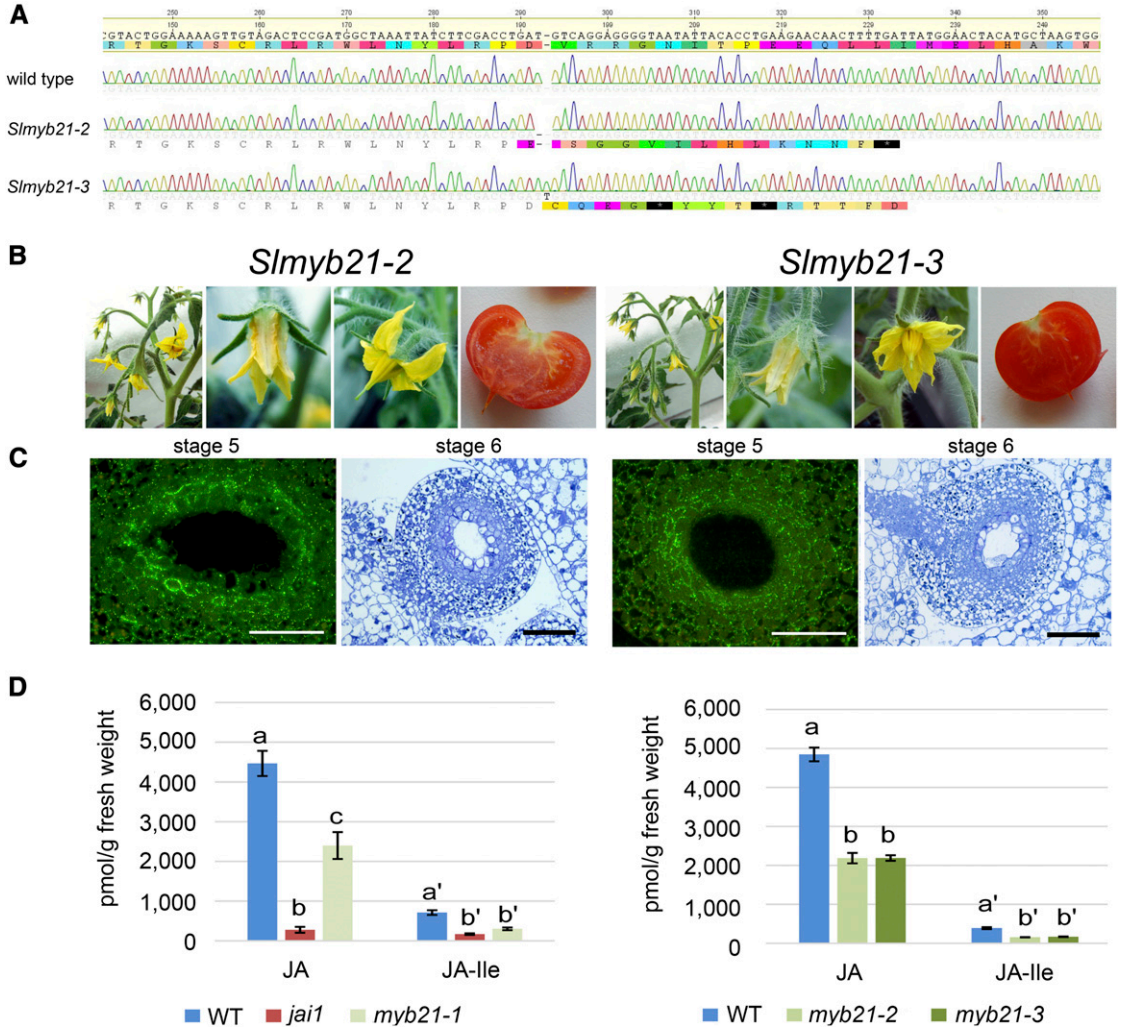

Figure 5. *Slmyb21-2* and *Slmyb21-3* Mutant Flowers and Fruits Show a Phenotype Similar to *jai1-1*, but Differ in the JA Content of Carpels.

(A) Sequence of genomic DNA encoding MYB21 showing the wild type (WT) sequence and two mutant sequences, which have either a deletion of one T (*Slmyb21-2*) or an insertion of one T (*Slmyb21-3*). The resulting peptide sequences are given below the DNA sequencing graph and show that both mutations result in a premature stop.

(B) Flowers of homozygous mutant plants exhibited defective opening and a protrusion of the stigma from the stamen cone of mature flowers. Fruits did not develop seeds.

(C) Cross-sections of mutant ovules show enhanced callose accumulation around and vacuolated cells in the inner layer of the nucellus as visualized by immuno stain at stage 5 and toluidine blue staining at stage 6, respectively. Bars = 50 μm in all micrographs.

(D) JA and JA-Ile levels in carpels of *Slmyb21* were diminished in comparison with wild type, but were higher than in *jai1-1* carpels. Carpels of stage 3 of wild type, *jai1-1*, and *Slmyb21-1* (left) as well as of wild type, *Slmyb21-2*, and *Slmyb21-3* (right) were extracted and contents of JA and JA-Ile were determined. Mean values ±SE are shown ($n = 5$ independent pools of carpels). Different letters within data for compound indicate significant differences according to one-way-ANOVA with Tukey's HSD test ($P < 0.05$).

jai1-1, and *Slmyb21-2*. The precursors GA_{12} and GA_{53} are oxidized in three steps in parallel pathways into GA_9 and GA_{20} by the GA 20-oxidases. The formation of the bioactive compounds is then catalyzed by GA 3-β-hydroxylases, whereas the activity of GA 2-oxidases leads to formation of inactive compounds (GA_{51}, GA_{34}, GA_{29}, GA_8; Hedden and Thomas, 2012). In tomato, the major GA-biosynthesis pathway is represented by the early 13-hydroxylation pathway synthesizing GA_1 as the bioactive form (García-Hurtado et al., 2012). The measurements revealed, however, enhanced levels of GA_4 in *jai1-1* in comparison with wild type. In addition, levels of inactive precursors GA_{53}, GA_{44}, and GA_{19} as well as of inactive catabolites GA_{34}, GA_{29}, and GA_8 was higher in *jai1-1* than in wild type, whereas the level of inactive intermediate GA_{20} was lower. The higher levels of GA_{53}, GA_{44}, and GA_{29} as well as the lower amount of GA_{20} might indicate decreased conversion of GA_{19} to GA_{20} and/or increased conversion of GA_{20} to GA_{29}. The latter correlates with the enhanced expression of a GA 2-oxidase (Figure 6E), which might also

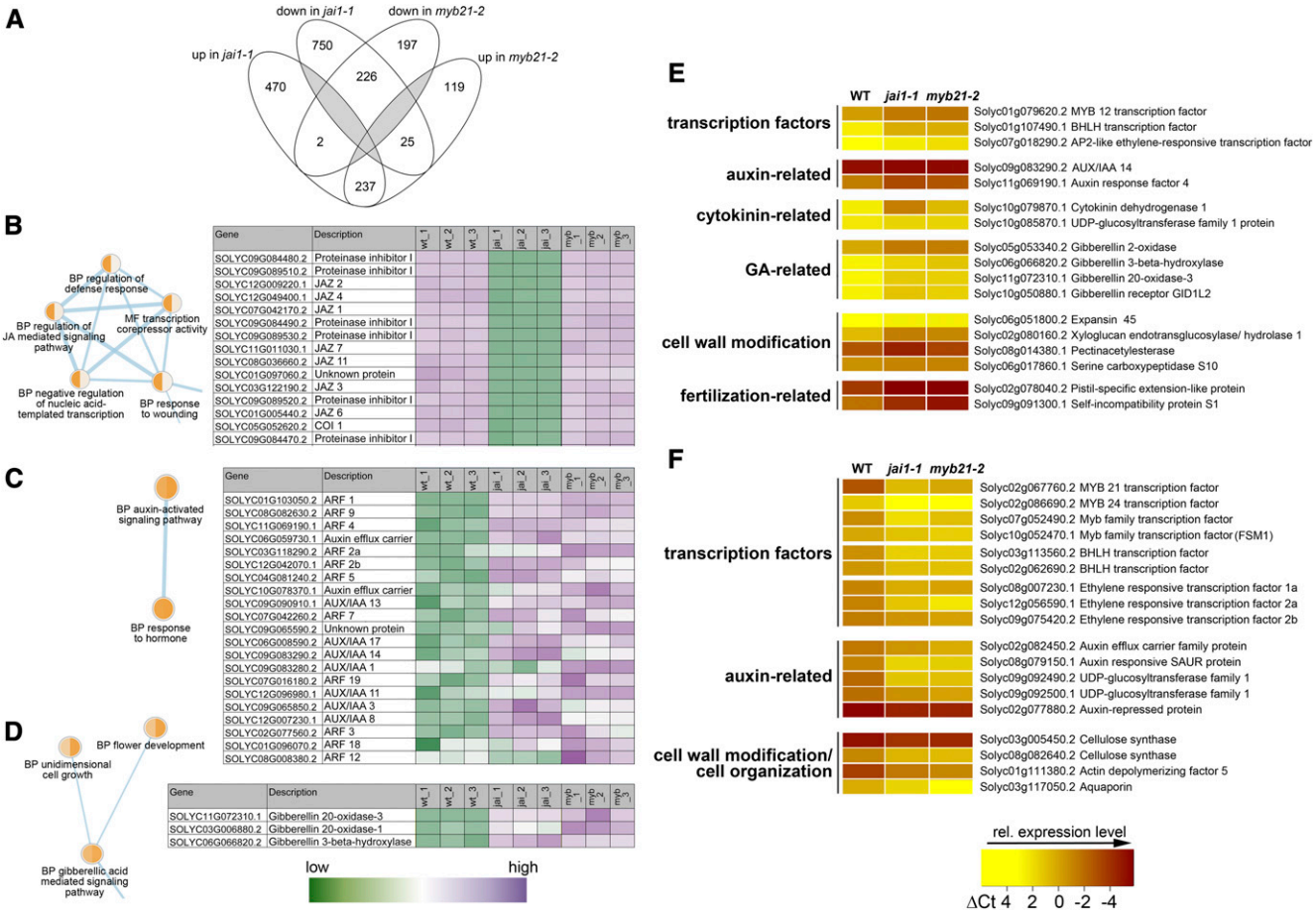

Figure 6. Comparative Analysis of Transcript Accumulation in Carpels at Flower Stage 3 of Wild Type (WT), *jai1-1,* and *slmyb21-2*.

Total RNA isolated from carpels at stage 3 of wild type, *jai1-1*, and *Slmyb21-2* was subjected to transcript profiling using RNA-seq.
(A) Venn diagram showing the number of significantly regulated genes ($P \leq 0.01$, $n = 3$ from different plants with two carpels pooled each) in both mutants in comparison with wild type. Note that the highest number of differentially regulated genes was found in *jai1-1*, and in both mutants 226 and 237 genes were commonly down- and upregulated, respectively.
(B) to **(D)** Classification of differentially expressed genes according to Gene Ontology: B: regulation of jasmonic acid–mediated signaling pathway, C: auxin-activated signaling pathway, D: gibberellic acid–mediated signaling pathway. Selected nodes (biological processes, BP) from the Enrichment Map where the left half corresponds to the comparison of *jai1-1* to wild type and the right half of *Slmyb21-2* to wild type are shown. Note that light orange symbolizes a high q-value and therefore almost no impact on the enrichment (see Supplemental Figure 7). The corresponding heat maps are based on the row-scaled expression values ($\log_2$ FPKM+1) and list the set of genes, which contributed most to the enrichment of the selected biological process.
(E) Relative transcript levels of genes commonly upregulated in *jai1-1* and *Slmyb21-2*.
(F) Relative transcript levels of genes commonly downregulated in *jai1-1* and *Slmyb21-2*. All transcript levels in **(C)** and **(D)** were determined by RT-qPCR and set in relation to *SlTIP41*. The color code visualizes the ΔCt values from yellow representing high values (= almost no transcripts detectable) up to red representing low values (= high expression). The calculated, relative transcript levels are given in Supplemental Tables 3 and 4.

contribute to the enhanced levels of GA_{34} in the parallel non–13-hydroxylation pathway (left side of the Figure 7).

Although showing similar gene expression data, carpels of *Slmyb21-2* exhibited similar GA levels as carpels of the wild type, except increased levels of GA_{53} and GA_{19}. Taken together, mainly GA intermediates representing precursors of bioactive GAs are increased in carpels of *Slmyb21-2* at stage 3 in comparison with carpels of wild type flower buds. This makes it rather unlikely that enhanced levels of bioactive GAs might be the reason for the enhanced biomass of *Slmyb21-2* carpels, whereas increased levels of GA_4 in *jai1-1* carpels might be causal for enhanced growth.

DISCUSSION

The survival of most plant species depends on flower development, successful fertilization, fruit, and seed set. All these processes require timely coordination between different organs by precise regulatory mechanisms that are, at least in part, mediated by phytohormones. For example, JAs are important for maintaining fertility, since the JA-insensitive mutants *coi1* (Arabidopsis) and *jai1* (tomato) are both sterile. However, like the great diversity in flower morphology and fruit variants between different species, the regulatory mechanisms seem to be different

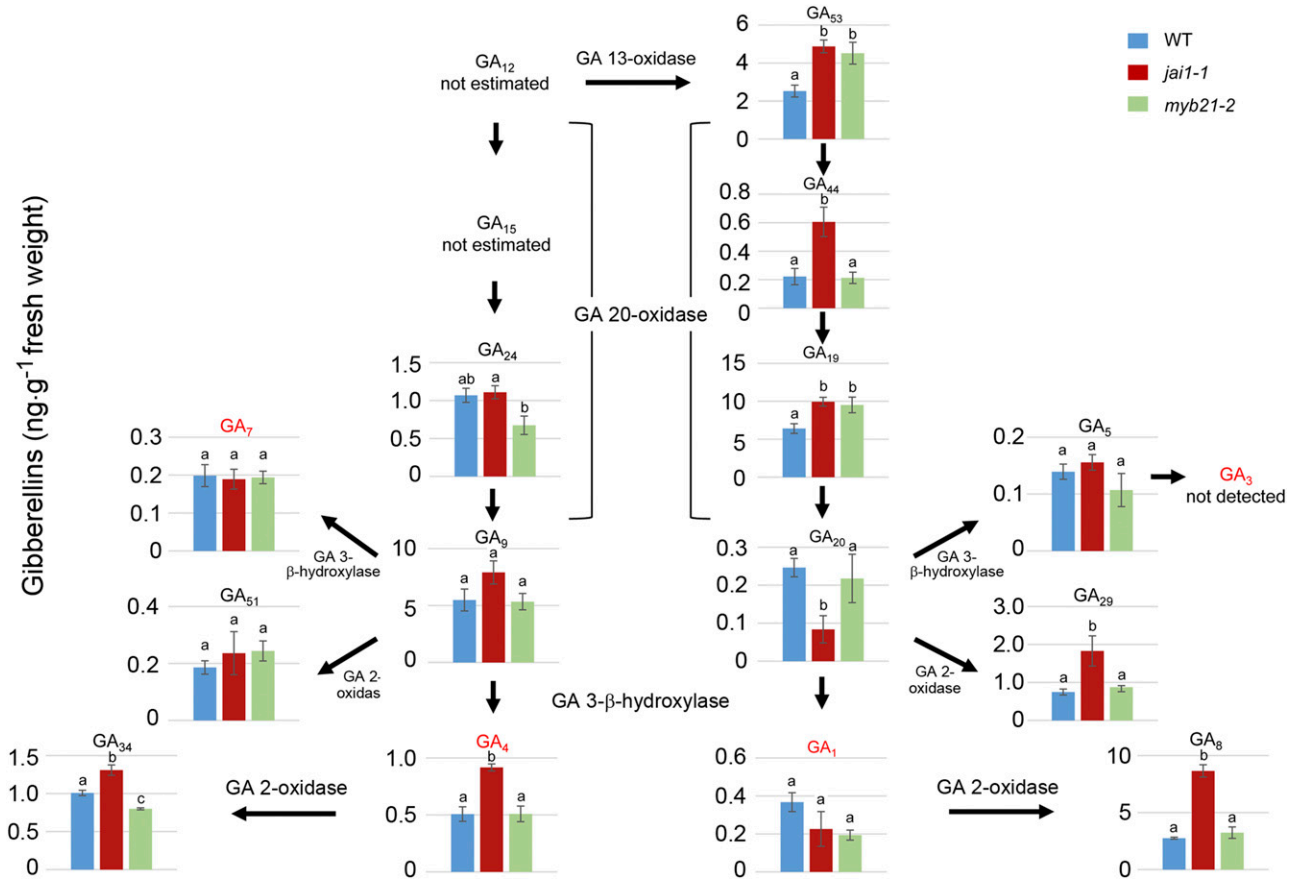

Figure 7. GA Levels in Carpels From Flower Buds at Stage 3 From Wild Type (WT), *jai1-1*, and *myb21-2*.

Simplified GA biosynthesis pathway and levels of 14 GA isoforms determined in carpels from flower buds at stage 3. Data are means ±SE ($n = 5$ independent pools of carpels). Different letters within data for each compound indicate significant differences according to one-way ANOVA with Tukey's Honestly Significant Difference test ($P < 0.05$).

regarding tissue-specific functions: the tomato *jai1* mutant is female sterile, whereas the Arabidopsis *coi1* mutant is male sterile. Here, we addressed the question of species-specific action of JA in flower development by dissecting its function in tomato ovule development.

JA/JA-Ile levels of carpels and ovules determined via hormone measurements and immunological detection, respectively, peaked in the biggest but still closed flower bud in wild type (stage 3). This contrasts with *jai1-1*, where JA and JA-Ile were not detectable in carpels and ovules (Figure 1). Stage 3 is the developmental stage shortly before flowers fulfill their reproductive function. Consequently, coordination of anther dehiscence, ovule maturation, and petal opening is required. The lack of JA perception in *jai1-1* ovules resulted in an abnormal development at later stages as visible by callose accumulation around cells of the inner layer of the nucellus accompanied by vacuolization of these cells (Figure 3). Both features are indicative of PCD, which was evidenced by a positive TUNEL assay in *jai1-1* ovules. This premature PCD leading to an early nucellus breakdown and putative disruptions in endosperm development (Xu et al., 2016) might be the reason for the impaired embryo development of *jai1-1* (Goetz et al., 2012). Indeed, comparative transcript analysis between wild-type and *jai1-1* ovules revealed that in comparison with wild type, several genes involved in peptide cleavage and polysaccharide-related cell wall modifications were significantly upregulated in *jai1-1* ovules dissected from open flower (Figures 2B and 2D). This indicates a negative regulatory role of JA in processes normally involved in cell death, which is induced after fertilization and has to be prevented before anthesis.

Regarding identification of putative mediators of the JA function, the transcriptomics data pointed toward *SlMYB21*, which was highly expressed in ovules from wild-type carpels at stage 3, but not at all in *jai1-1* ovules. Its ortholog AtMYB21 is involved in JA-regulated filament and petal elongation in Arabidopsis (Mandaokar et al., 2006; Song et al., 2011; Reeves et al., 2012). Therefore, SlMYB21 was a promising candidate to be a putative mediator of JA function in tomato ovule development. Similarly to AtMYB21, expression of *SlMYB21* is strictly JA dependent and specific to flowers, and the protein interacts with JAZ9 (Figure 4). The control of MYB21 protein activity by JA via a JAZ protein might lead to an even stronger

loss-of-function in the JA-insensitive mutant due to the missing JA-induced degradation of JAZ proteins. To confirm that SlMYB21 is functionally equivalent to AtMYB21, *SlMYB21* was expressed under the control of the *AtMYB21* promoter in the Arabidopsis mutant *myb21-5* (Reeves et al., 2012). This expression led to a complementation with respect to petal length and flower opening, but filament elongation showed varying results ranging from filaments that were slightly longer than those of *myb21-5* (above sepal length) until complete rescue in two lines. Interestingly, such a partial, varying rescue is also achieved by complementation with the genomic sequence of *AtMYB21* itself (Figure 4F) suggesting a complex regulation of *MYB21* expression. Moreover, these results point to a different regulation of *MYB21* expression in petals and stamen of Arabidopsis. Nevertheless, the same partial rescue visible with *MYB21* from Arabidopsis and tomato supports the homology of the two MYB21 proteins.

The functional characterization of SlMYB21 and elucidation of its role in mediating JA function in tomato flower development were performed by identification of a TILLING mutant and generation of two independent mutants by CRISPR/Cas9 genome editing. All three mutants revealed a SlMYB21 function in flower buds and open flowers starting at the developmental stage 3. The mutant buds were bigger than those from wild type (Supplemental Figure 6), and the petals failed to open properly, even more severely than in *jai1-1*, indicating a JA-independent function of MYB21 in petal opening. Also, contrasting with the phenotype of *jai1-1*, there was no early senescence of stamen and hardly any impairment of pollen viability in *Slmyb21-2* (data not shown; Li et al., 2004; Dobritzsch et al., 2015), supporting a MYB21-independent role of JA in the process of stamen and pollen development in tomato. This is different to tomato plants expressing an artificial repressor, *AtMYB24-SUPERMAN REPRESSION DOMAIN X*, which was expected to impede the function of SlMYB21 and did result in flowers with aborted flower opening, but additionally exhibited abnormal pollen grains (Niwa et al., 2018). Moreover, we found that SlMYB21 acts as a positive regulator of JA biosynthesis as shown by the diminished JA/JA-Ile levels in all three *Slmyb21* mutants. This contrasts with AtMYB21, which acts as a negative regulator of JA biosynthesis, because of increased JA levels in flowers of *Atmyb21 myb24* double mutants, which in turn result in enhanced transcript levels of *JAZ* genes, *LIPOXYGENASE2, LIPOXYGENASE4, ALLENE OXIDE SYNTHASE*, and *OPDA REDUCTASE3* (Reeves et al., 2012; Huang et al., 2017).

The development of carpels and ovules in the *Slmyb21* mutants was very similar to *jai1-1* as indicated by the size of carpels and the morphology of ovules, which accumulated callose and showed vacuolated cells in the innermost cell layer of the nucellus (Figure 5; Supplemental Figure 5). It is tempting to speculate that JA acts through SlMYB21 to prevent nucellus senescence processes before anthesis. Surprisingly, however, *Slmyb21-2* plants were able to develop a few seeds after hand pollination performed before flower opening, suggesting that the obvious defects in ovule development of *Slmyb21* mutants are not as severe as in *jai1-1*. Thus, we hypothesized that defects in MYB21 protein function led to an uncoupling of fertilization and fruit development, since under normal conditions *Slmyb21-2* and *Slmyb21-3* plants produced fruits similarly to wild type but did not develop seeds.

To gain insight into how the development of tomato carpels is regulated by JA and MYB21, a comparative transcript profiling was performed using wild type, *jai1-1*, and *myb21-2* carpels from flower buds at stage 3. The commonly deregulated genes in both mutants contained gene groups related to GA-biosynthesis and auxin signaling (Figures 6C to 6F). Both hormones are known to be essential signaling molecules mediating the switch from flower to fruit development, since exogenous application of both hormones initiates fruit set without fertilization (Serrani et al., 2007). On the one hand, a strong interference with the auxin homeostasis regulation became obvious–several AUX/IAA proteins and auxin response factors (ARFs) encoding genes were upregulated in carpels of both mutants, among them, *ARF5* and *ARF7* known to act as regulators for fruit set (de Jong et al., 2009; Liu et al., 2018) and *ARF9* known to be induced after fertilization or after auxin treatment (de Jong et al., 2015). Their upregulation might contribute to the formation of parthenocarpic fruits, which were also found upon downregulation of the ARF7 repressor *IAA9* (Wang et al., 2009). Therefore, the formation of parthenocarpic fruits might at least in part be due to the loss of fine-tuned auxin signaling.

GAs represent another important signal in flower and fruit development. GA levels increase in the ovary upon pollination (Gorguet et al., 2005; Serrani et al., 2007) and a constitutive GA signaling results in parthenocarpic fruits (Carrera et al., 2012). Our data point to a negative feedback of JA and MYB21 on expression of GA-biosynthetic genes in carpels of closed flower buds (Figures 6D and 6E) and indicate a GA-mediated signaling in mutant buds that is similar to wild-type flowers after fertilization. The levels of bioactive GAs were, however, not elevated in carpels of *jai1-1* and *myb21-2* except that a higher content of GA_4 was observed in *jai1-1* (Figure 7). In tomato, the early 13-hydroxylation pathway leading to the bioactive form GA_1 is the major GA-biosynthetic pathway. It was reported, however, that overexpression of *GA 20-oxidases* shift the metabolism to the parallel non–13-hydroxylation pathway, resulting in biosynthesis of GA_4 (García-Hurtado et al., 2012). The increased transcript levels of *GA 20-oxidases* in carpels of *jai1-1* might therefore cause the accumulation of GA_4.

GA and auxin commonly regulate fruit initiation by the interplay of the GA-signaling repressor SlDELLA and auxin-signaling components, such as SlIAA9 and SlARF7, which together repress parthenocarpy by coregulation of genes involved in fruit growth and, additionally, GA and auxin metabolism (Hu et al., 2018). Therefore, fine-tuning of auxin and GA signaling seems to be essential for controlling the signal for switching from flower into fruit development. The deregulation of GA and auxin signaling in carpels of *jai1-1* and *myb21-2* flower buds at stage 3 points toward a negative regulatory role of JA and MYB21 on GA and auxin action, thereby preventing fruit initiation before fertilization (Figure 8). This was clearly visible in both mutants by the early ovary growth (Supplemental Figures 1 and 6) as well as by the up- and downregulation of genes that are involved in cell separation and in cell shape maintenance, respectively (Figures 6E and 6F).

In summary, MYB21 mediates JA function mainly during carpel and ovule development in tomato, but is additionally involved in the coordination of flower opening (Figure 8). In doing so, there

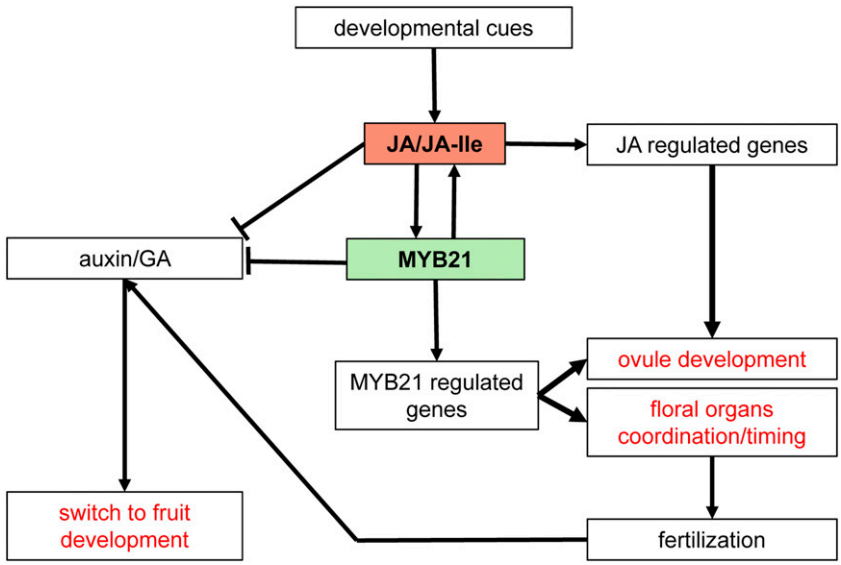

Figure 8. Jasmonates and SlMYB21 Regulate Ovule Development in Tomato.

During flower development in tomato, levels of JA and JA-Ile increase transiently resulting in upregulation of JA-regulated genes including this encoding SlMYB21, which in turn regulates specific genes. In addition, action of SlMYB21 positively feed back into JA/JA-Ile biosynthesis. Both JA- and MYB21-regulated gene expression are necessary to ensure proper ovule development and contribute to coordination of floral organ development. In addition, JA/JA-Ile and SlMYB21 repress biosynthesis and/or function of auxin and GA, thereby preventing a premature switch into fruit development.

seems to be conserved functions of MYB21 during petal development and flower opening in Arabidopsis and tomato. Regarding the development of reproductive organs, however, tomato MYB21 might function as a hub in the interplay of JA, auxin and GA in the carpel by coordination of the timely death of the nucellus after fertilization and the initiation of fruit formation, both being essential for successful seed set and development.

METHODS

Plant Material, Growth Conditions, Harvest of Carpels, and Dissection of Ovules

Tomato (*Solanum lycopersicum*) plants cv MicroTom wild type, *jai1-1* (Li et al., 2004), and mutants generated during this work were grown in a controlled growth chamber with 16 h light (200 μmol photons*m^{-2}*s^{-1}; Metal Halide Lamp MT250DL, IWASAKI Electric Co.) at 26°C and 8 h dark at 20°C, both at 70% humidity. Homozygous *jai1-1* mutants were selected by PCR according to (Li et al., 2004). Phenotypic markers such as missing anthocyanin production in first leaves and protrusion of stigma were additionally used.

Harvest of carpels was performed using 5- to 6-week-old plants showing the first open flowers. Carpels of defined developmental stages were harvested in a very strict time window of 30 min starting at 7 h after the onset of light period, collected on dry ice, transferred to liquid nitrogen, and stored at −80°C. Carpels of primary inflorescences were used for dissecting ovules. Hand-cut sections of carpels were transferred immediately into ice-cold ethanol and vacuum infiltrated. Ovules were dissected using a stereomicroscope and stored in ethanol at −20°C. After freeze drying at −20°C for 4 h, material was directly used for RNA isolation. Harvesting time for carpels subjected to phytohormone quantification was expanded to 2 h, and carpels of primary and secondary inflorescences were used.

Determination of Fresh and Dry Weight, and Calculation of Water Content

Carpels were harvested and fresh weight (FW) was determined immediately. After drying at 50°C for one week, the dry weight was determined and the water content (WC) calculated according to the formula: WC = (FW − dry weight)/FW.

Determination of JA, JA-Ile, and GAs

Quantitative analysis of JA and JA-Ile was done using 50 mg of homogenized plant material per sample as described (Balcke et al., 2012). In brief, plant material was extracted with 500 μL pure methanol supplied with [$^2H_6$]JA, and [$^2H_2$] JA-Ile (50 ng each) as internal standards. After centrifugation, the supernatant was diluted with 9 volumes of water and subjected to solid phase extraction on HR-XC (Chromabond, Macherey-Nagel) column. Elution was done with 900 μL acetonitrile. Ten μL of the eluate were subjected to ultraperformance liquid chromatography–tandem mass spectrometry according to Balcke et al. (2012). The contents of JA, and JA-Ile were calculated using the ratio of analyte and internal standard peak heights.

Samples were analyzed for GA content according to Urbanová et al., 2013 with some modifications. Carpels of stage 3 from wild type, *jai1-1*, and *myb21-2* (30 mg of fresh weight) were homogenized with 1 mL 80% (v/v) acetonitrile containing 5% (v/v) formic acid and 19 internal GA standards ([$^2H_2$]GA_1, [$^2H_2$]GA_3, [$^2H_2$]GA_4, [$^2H_2$]GA_5, [$^2H_2$]GA_6, [$^2H_2$]GA_7, [$^2H_2$]GA_8, [$^2H_2$]GA_9, [$^2H_2$]GA_{12}, [$^2H_2$]GA_{12}ald, [$^2H_2$]GA_{15}, [$^2H_2$]GA_{19}, [$^2H_2$]GA_{20}, [$^2H_2$]GA_{24}, [$^2H_2$]GA_{29}, [$^2H_2$]GA_{34}, [$^2H_2$]GA_{44}, [$^2H_2$]GA_{51} and [$^2H_2$]GA_{53}; OlChemIm) and extracted at 4°C overnight with constant stirring. The homogenates were centrifuged for 10 min at 4°C, and supernatants were purified using mixed mode anion exchange cartridges (Waters, www.waters.com). Analysis was done by ultra-high-performance liquid chromatography (Acquity UPLC System; Waters) coupled to triple-stage quadrupole mass spectrometer (Xevo TQ MS, Waters) equipped with electrospray ionization interface. GAs

were detected using multiple-reaction monitoring mode based on transition of the precursor ion $[M-H]^-$ to the appropriate product ion. Data were acquired and processed by Masslynx 4.1 software (Waters), and GA levels were calculated using the standard isotope-dilution method (Rittenberg and Foster, 1940).

Histochemical Analyses

For light microscopic analysis carpels were fixed in 3% (v/v) sodium cacodylate-buffered glutardialdehyde (pH 7.2), dehydrated in an ethanol series, and embedded in epoxy resin (Spurr, 1969). Semi-thin sections (1 μm) were stained with toluidine blue. To stain callose, sections were treated with 0.5% (w/v) NaOH in ethanol for 5 min followed by two washing steps with water. Immunostaining was done using a mouse anti-(1→3)-β-glucan antibody (Biosupplies, http://www.biosupplies.com.au/, Cat# 400-2) diluted 1:500 in phosphate buffer saline (PBS) containing 5% (w/v) BSA at 4°C overnight followed by a goat-anti-mouse-IgG antibody conjugated with AlexaFluor488 (Invitrogen, www.thermofisher.com/ý) at 37°C for 90 min. Sections were mounted in anti-fading reagent Citifluor (Science Services GmbH).

For immunocytochemical analysis of JAs, carpels were fixed with 4% (w/v) 1-ethyl-3-(3-dimethyl aminopropyl)-carbodiimide hydrochloride (Merck KgaA) in PBS, embedded in polyethylene glycol (PEG) 1500, and immunostained with an antibody against JA as described (Mielke et al., 2011).

Fixation of carpels with 4% (w/v) paraformaldehyde/0.1% (v/v) Triton X-100 in PBS and embedding in paraplast (Sigma-Aldrich) was used for TUNEL. The 12-μm-thick sections were pretreated with 2 μg mL^{-1} proteinase K in 10 mM Tris-HCl (pH 8.0) at 37°C for 30 min. After washing with PBS, TUNEL reaction was carried using the in situ Cell Death Detection Kit (Sigma-Aldrich) according to the supplier's instructions. Positive controls were generated by pretreatment of sections with 1 μg mL^{-1} DNase I in PBS at room temperature for 10 min. Negative controls were obtained by omitting the terminal-deoxynucleotidyl-transferase. After washing, sections were mounted in the anti-fading reagent Citifluor.

Micrographs were taken using a Zeiss 'AxioImager' microscope (Zeiss) equipped with an AxioCam (Zeiss) and were combined using Photoshop 12.0.4 (Adobe Systems).

RNA Isolation and RT-quantitative PCR

RNA isolation from homogenized material was performed using the RNeasy Plant Mini Kit (Qiagen, www.qiagen.com) according to the supplier's instructions including on-column digestion of DNA for 30 min or routine DNase treatment using DNA-free Kit (Thermo Scientific, /www.thermofisher.com/) afterward. RNA quality was tested by capillary electrophoresis using QIAxcel Advanced System (Qiagen). First strand cDNA synthesis was performed in a final volume of 20 μL with M-MLV Reverse Transcriptase, RNase H Minus, Point Mutant (Promega, /www.promega.de/) or ProtoScript II First Strand cDNA Synthesis Kit (NEB, /www.neb-online.de/) according to the supplier's protocol using oligo (dT)19 primer.

The 3 μL of diluted cDNA was mixed with 2 μL 5x EvaGreen QPCR Mix II (Bioandsell), 2 pmol forward primer, and 2 pmol reverse primer and dH_2O (ad 10 μl). QPCR primers for candidate genes were designed with the software CloneManager (Sci-Ed Software) and Primer3 (http://bioinfo.ut.ee/primer3/) using the corresponding sequences of the tomato genome (sol genomic network, http://solgenomics.net and GeneBank, https://www.ncbi.nlm.nih.gov/genbank/; for primer sequences see Supplemental Table 4). PCR was done using RT-qPCR-System CFX Connect (Bio-Rad, www.bio-rad.com) with the following protocol: denaturation (95°C for 15 min), amplification (40 cycles of 95°C for 15 s and 56°C for 30 s), and melting curve (95°C for 10 s, 60°C heating up to 95°C with a heating rate of 0.05°C s^{-1}). Data were analyzed with CFX Manager Software (Bio-Rad). Relative gene expressions were calculated by the comparative quantitation cycle method (Schmittgen and Livak, 2008) using *S. lycopersicum TAP42 INTERACTING PROTEIN* (*SlTIP41*; Expósito-Rodríguez et al., 2008) as constitutively expressed gene. Each reaction was measured in duplicate or triplicate.

Transcript Profiling using GeneChip Analysis

RNA isolated independently from three ovule samples per developmental stage (1, 3, and 6), all from wild type and *jai1-1*, was analyzed using Agilent-Tomato 44K-full genome chips. Synthesis and purification of cDNA; synthesis, labeling, purification, quality control, and fragmentation of coding RNA; as well as hybridization, washing, and scanning of the chips were done by the service partner Atlas Biolabs (http://www.atlas-biolabs.de/) according to the supplier's protocols.

Data analysis was performed using ArrayStar (www.dnastar.com). All samples were quantile normalized. To identify genes that were differentially expressed, pairwise comparison between wild type and *jai1-1* at the three different developmental stages was done. P-values were corrected according to the Benjamini-Hochberg method using the statistical package of ArrayStar. Genes were considered as differentially expressed when adjusted p-values were ≤ 0.01 and fold change ≥ 8. Sets of gene showing differential expression were obtained for each developmental stage. Gene annotation was done using data from 'sol genomic network' and mapping results obtained by MapMan (www.mapman.gabipd.org) followed by manual check and correction using nucleotide BLAST (www.ncbi.nlm.nih.gov).

Transcript Profiling using Illumina Sequencing

RNA isolated from carpels of stage 3 from wild type, *jai1-1*, and *myb21-2* was used for Illumina sequencing. A 1 μg subsample of total RNA from each of 9 RNA extracts (1 stage×3 genotypes×3 biological replicates) was sent to the GATC Biotech AG (https://www.eurofinsgenomics.eu/) and used to produce Illumina HiSeq 2500 strand-specific 2×150 bp paired-end reads. Total RNA quality was determined using an Agilent 2100 Bioanalyzer, and quality of the sequenced raw reads were assessed by FastQC (version 0.11.5, http://www.bioinformatics.babraham.ac.uk/projects/fastqc/).

Read adapters were removed with cutadapt (version 1.16), and quality trimming was performed with sickle (version 1.33). Cleaned reads were mapped by STAR (–alignIntronMin 40–alignIntronMax 5000, version 2.5.2) against the reference genome assembly of tomato SL2.50 downloaded from the Plant ENSEMBL database. Gene counts were obtained with subread's featureCounts (version 1.5.1) by counting unique exonic overlaps. The reproducibility of the biological replicates was confirmed by hierarchical clustering using the 1-correlation (spearman) as distance measures between samples. For detecting differential gene expression edgeR was used to perform likelihood ratio test on the linear models. Library sizes were scaled using the TMM method in egdeR, and dispersion was estimated tagwise (genes). Low expressed genes with counts per million (cpm) < 1 within each replicate group were excluded from statistical analysis. P-values were adjusted using Benjamini and Hochberg false discovery rate procedure. Differently expressed genes were identified by a significance threshold of 0.05 and a minimal log2-fold-change of ±1.

Further analysis by enrichment of Gene Ontology terms was performed based on gene set enrichment analysis (Subramanian et al., 2005) using the enrichment map app from Cytoscape (Merico et al., 2010) with a false discovery rate–q-value and similarity cutoff of 0.15 and 0.3, respectively.

Cloning of *MYB21* and JAZ-Encoding Genes for Interaction Studies

Gateway recombination was used for Y2H and BiFC approaches. Therefore, PCR was performed with AccuPrime Pfx SuperMix (Invitrogen) and

primers containing *attB1/B2* sites using cDNA from tomato shoot material treated with JA-methyl ester to amplify *JAZ1, JAZ2, JAZ6, JAZ7, JAZ8, JAZ9, JAZ10*, and *JAZ13*. For amplifying the coding sequence (CDS) of *JAZ3, JAZ4, JAZ11, MYB21*, and *JAZ5*, cDNA from stamen and JA-methyl ester-treated root material, respectively, was used. The PCR products were cloned into vector pDONR221-P1P2 and pDONR221-P1P4/P3P2 for Y2H and BiFC, respectively, using the BP-Clonase Kit II (Invitrogen). Primer pairs for the construction of the entry vectors are listed in Supplemental Table 5.

For Y2H, all JAZ coding sequences were fused to DNA BD and MYB21 CDS to AD of GAL4 by recombination into pDEST32 and pDEST22 (Invitrogen), respectively. BiFC binary vectors were achieved using 2in1 vectors according to Grefen and Blatt, 2012. For splitTALE assay (Schreiber et al., 2019), the CDS of MYB21 with or without AD (C-terminal deletion of 25 aa) and JAZ9 were cloned into level 1 vectors using Golden Gate method (Werner et al., 2012), resulting in a fusion either to the TALE BD (N-terminal; *Act2p:TALE(BD)-MYB21*) or to AD (C-terminal; *35S:JAZ9-TALE[AD]*; Schreiber and Tissier, 2016). For splitTALE assays, constructs were transformed into *Agrobacterium tumefaciens* strain *GV3101* and used for transient expression in *Nicotiana benthamiana* leaves.

Primer pairs are listed in Supplemental Table 6. All constructs were transformed into *Escherichia coli* strain *DH10B*, from which plasmids were isolated using a plasmid isolation kit (Macherey-Nagel).

Transcriptional Activation Analysis in Yeast Cells

For testing the transcriptional activity of MYB21, its CDS was fused to GAL4 BD into pDEST32. Yeast transformation was performed as described below, and pDEST22 was added as an empty vector. Transcriptional activity was deduced from yeast growth on synthetic defined (SD) medium –Trp/-Leu/-His (plus 2 mM 3-amino-1,2,4-triazol).

Yeast-Two-Hybrid Assays

Transformation of competent pJ69 yeast cells was done as described previously (Gietz and Schiestl, 2007). Yeast cells were incubated with bait and prey plasmids, PEG 3350, 0.1 M lithium acetate, and single-stranded carrier DNA at 42°C for 1 h. Yeast cells were grown for 6 d on SD medium -Trp/-Leu. Single colonies were selected and cultured overnight at 30°C to an OD_{600} of 1, harvested, and resuspended in sterile water. The 5 μL of undiluted and 1:10 and 1:100 diluted suspensions were dotted either on SD medium -Trp/-Leu or on SD medium -Trp/-Leu/-His (plus 2 mM 3-amino-1,2,4-triazol) and incubated at 30°C for 3 d. Cells grown on SD medium -Trp/-Leu/-His were indicative for an interaction of the proteins under study.

BiFC in *N. benthamiana* Protoplasts

Plasmid DNA was isolated from 50 mL *E. coli* overnight culture using the PureYield Plasmid Midiprep Kit (Promega). DNA purification was done by filtration, precipitation using PEG, washing with 70% (v/v) ethanol, and resolving in 20 μL water. Protoplast transformation was done according to Yoo et al., 2007 with some modifications. Protoplasts were isolated from two young leaves of 4-week-old *N. benthamiana* plants that were cut in small pieces and vacuum infiltrated with 5% (w/v) cellulase Onozuka R-10 and 0.4% (w/v) macerozyme R.10 (both from Yakult, www.yakult.co.jp/ypi/en/) in 0.4 M mannitol, 20 mM KCl, 20 mM MES (pH 5.7), 110 mM $CaCl_2$, and 0.1% (w/v) BSA, and incubated for 4 h followed by shaking for 30 min. The cells were directly passed through a nylon mesh filter, the flow-through centrifuged for 1 min at 200 g, and resuspended first in W5 (154 mM NaCl, 125 mM $CaCl_2$, 5 mM KCl, 2 mM MES, pH 5.7) and finally in mannitol-magnesium buffer (0.4 M mannitol, 15 mM $MgCl_2$, 4 mM MES, pH 5.7) to get a density of 10^5 protoplasts per mL. For transformation, 200 μL of protoplast suspension were incubated with 10 μg plasmid and 40% (w/v) PEG in 0.2 M mannitol and 100 mM $CaCl_2$ for 5 min. After sedimentation at 200 g for 1 min, cells were resuspended in 200 μL W1 buffer (0.5 mM mannitol, 20 mM KCl, 4 mM MES, pH 5.7) and incubated at room temperature overnight. Images were captured by a Confocal Laser Scanning Microscope (LSM700, Zeiss). Upon excitation of 488 nm, yellow fluorescent protein fluorescence and chlorophyll autofluorescence were recorded at 493-531 nm and 644-800 nm, respectively.

SplitTALE Assays in *N. benthamiana*

Overnight cultured Agrobacteria transformed with the respective plasmids were resuspended in infiltration media consisting of 10 mM MES, 10 mM $MgCl_2$, and 100 μM acetosyringone to $OD_{600} = 0.4$. Agrobacteria containing the splitTALE constructs and the reporter construct *4xSTAP1:GUS* (Schreiber and Tissier, 2016; Schreiber et al., 2019) were mixed in ratio 1:1:1 and used to transiently transform *N. benthamiana* leaves through syringe-mediated infiltration (Sparkes et al., 2006). At 3 d after inoculation, leaf material was harvested, frozen in liquid nitrogen, homogenized, and mixed with extraction buffer containing 50 mM Na_2HPO_4 (pH 7), 10 mM EDTA, 0.1% (w/v) SDS, 0.1% (v/v) Triton X-100, and 10 mM β-mercaptoethanol. GUS assay was performed as described (Kay et al., 2007). GUS activity was measured after incubation with 4-methylumbelliferyl-β-D-glucuronide trihydrate (Duchefa, www.duchefa-biochemie.com) at 37°C for 85 min and calculated in relation to the total content of proteins determined by Bradford method (Bradford and Trewavas, 1994).

Subcellular Localization in *N. benthamiana*

For localization studies, the Golden Gate method (Weber et al., 2011; Werner et al., 2012; Engler et al., 2014) was used to clone the genomic sequence of *MYB21* with the second intron shortened (2204 bp deleted) with a C-terminal GFP fusion under the control of *35S* promoter in level 1 vector (see primer pairs in Supplemental Table 6). The construct was infiltrated in *N. benthamiana* leaves mediated by *A. tumefaciens GV3101 pMP90* (OD_{600} = 0.5). Pictures were taken 3 d after infiltration using AxioImager (Zeiss) equipped with the proper filters for GFP and an AxioCam camera (Zeiss). The infiltrated area was harvested, and total protein extracted (Meyer et al., 1988) and subjected to SDS-PAGE followed by immunoblot analysis according to standard protocols. Immunodetection was performed with an anti-GFP antibody (Santa Cruz Biotechnology, https://www.scbt.com) as primary antibody and anti-mouse IgG conjugated with alkaline phosphatase (EMD Millipore Corporation) as secondary antibody. Immunodecorated GFP protein was stained with p-nitroblue tetrazoline chloride and 5-bromo-4-chloro-3-indolylphosphate.

Cloning of CRISPR/ Cas9 and Complementation Construct

Constructs were designed harboring two single guide RNAs targeting two specific 20-bp sequences (chosen using CRISPRdirect crispr.dbcls.jp) in the second exon of *MYB21* under the control of the Arabidopsis (*Arabidopsis thaliana*) *U6* consensus promoter (Nekrasov et al., 2013). All cloning steps were done using Golden Gate method (Werner et al., 2012; Engler et al., 2014). All cloning cassettes including the *Cas9* endonuclease CDS (Nekrasov et al., 2013) under the control of *35S* promoter were assembled into the level 2 vector pAGM4723.

For the complementation of *myb21-2*, a sequence of 1.5 kb upstream of the ATG start codon was cloned to drive the expression of *MYB21* (genomic sequence with shortened second intron) with a C-terminal fusion to a 3x*Flag* tag. All cloning cassettes were assembled into the level 2 vector pAGM4673. The constructs were finally used for transformation of *A. tumefaciens GV3101* followed by stable tomato transformation. All primer pairs are listed in Supplemental Table 6.

Stable Tomato Transformation

Tomato was stable transformed via somatic embryogenesis using cotyledon pieces of 8-d-old seedlings germinated on phytoagar (Duchefa) for 6 d in darkness and 2 d under 16 h photoperiod. The cotyledon pieces with 2 cutting sites were placed upside down on KCMS media (pH 5.7; 4.4 g/L MS including vitamins, 20 g/L Suc 200 mg/l KH_2PO_4, 8 g/L agar [Sigma-Aldrich], 0.9 mg/l thiamine, 100 μg/L kinetin, 0.5 mg/l IAA) and preconditioned overnight in the dark (Čermák et al., 2015). Overnight cultures of Agrobacterium were pelleted and resuspended in KCMS liquid-media (4.4 g/L MS including vitamins, 20 g/L Suc, 200 mg/l KH_2PO_4) to OD_{600} = 0.08 and used for transformation according to Fernandez et al., 2009. After 2 d in the dark, cotyledon pieces were transferred to 2Z-media with the abaxial side in contact to the media (4.4 g/L MS including vitamins, 30 g/L Suc, 100 mg/l myoinositol, 8 g/L agar, 1 mL/l Nitsch-vitamins [1000×; Duchefa], 375 mg/l timentin [ticarcillin and clavulanate 15:1; Duchefa], 100 mg/l kanamycin, 0.1 mg/l IAA, 2 mg/l trans-zeatin riboside; pH 5.8) and cultivated in 16-h photoperiod at 24°C. Developing calli and plantlets were transferred every 2 weeks to Z-media containing decreased trans-zeatin riboside concentrations from 1 to 0.5 mg/l and finally 0.1 mg/l GA instead of trans-zeatin riboside (Eck et al., 2006). After another 2 weeks on rooting media (4.3 g/L MS without vitamins, 30 g/L Suc, 100 mg/l myoinositol, 7 g/L agar, 1 mL/l Nitsch-vitamins, 375 mg/l timentin, 100 mg/l kanamycin), plants with developed roots were transferred into soil and slowly adjusted to 70% of relative humidity.

Generation and Characterization of Transgenic Arabidopsis Plants

The genomic sequence of *MYB21* of tomato (second intron shortened at 2204 bp) and Arabidopsis was amplified from genomic DNA using primers containing attB1/B2 sites and cloned into pDONR221 to generate entry vectors attR1-*MYB21*genomic-attR2. A 7281-bp region upstream of the start codon of the *AtMYB21* gene was cloned in pUC57-L1-KpnI-XmaI-R1, a pUC57 vector carrying KpnI and XmaI restriction sites between attL4 and attR1 sites for Gateway cloning (Invitrogen); this vector was kindly provided by the group of Niko Geldner in the University of Lausanne. The sequence immediately upstream of the AtMYB21 start codon is AT rich, impairing primer design. Therefore, the first six upstream nucleotides (a string of six adenines) were excluded from cloning. PCR amplification of the entire 7281 bp was unsuccessful; therefore, the region was cloned in two steps. First, primers P230+P194u amplified a 2277-bp region containing an endogenous KpnI restriction site at the 5′-end. The fragment was digested with KpnI and XmaI and cloned into pUC57-L1-KpnI-XmaI-R1 to generate pMP60. Second, primers P231+P197u amplified a 5558-bp fragment that overlaps by 546 bp with the insert in pMP60. This fragment was digested with KpnI and ligated to KpnI-linearized pMP60 to generate pMP71, the final pENTRY attL4-*MYB21*pro-attR1. The sequences cloned in pMP60 and pMP71 were confirmed by Sanger sequencing. The corresponding entry vectors were used for further recombination into pDG27 with *OLE1-tagRFP* for transformant selection (Shimada et al., 2010). The resulting binary vectors were used to transform *A. tumefaciens* strain *GV3101* to mediate the transformation of Arabidopsis *myb21-5* (Reeves et al., 2012) heterozygous plants by the floral dip method (Clough and Bent, 1998). All primer pairs are listed in Supplemental Table 7.

Transformed seeds were identified by checking for red fluorescence due to *OLE1:tagRFP* expression. Segregating homozygous *Atmyb21-5* lines were selected by using a cleaved-amplified polymorphic sequence marker for the mutant single nucleotide polymorphism. For this, the PCR products (see primer pair Supplemental Table 8) were digested with EcoRI (high fidelity, NEB) for 2 h.

Mutant Screen by TILLING

Lines mutated in the gene encoding MYB21 (*Solyc02g067760*) were screened from 9216 EMS-mutagenized lines by TILLING using LI-COR DNA analyzer according to the procedure described by Okabe et al., 2011. A 606-bp region encompassing the first two exons of the gene were amplified by PCR using the fluorescent DY-681- and DY-781-labeled primers (Biomers; Supplemental Table 9).

Genotyping of *Slmyb21* Tomato Mutants

PCRs were performed using Phire Plant Direct PCR Master Mix (Thermo Scientific) with 0.3-mm leaf discs as template. To select m*yb21* TILLING mutants cleaved-amplified polymorphic sequence markers (http://helix.wustl.edu/dcaps/dcaps.html) were used to identify the wild-type single nucleotide polymorphisms. The *SlMYB21* PCR products were digested using HphI for line TOMJPE7979 and Eco31I for *Slmyb21-1* (fast digest, Thermo Fisher Scientific). TILLING mutant line TOMJPE8245 was genotyped by high-resolution melt curve qPCR (from 60° to 90°C each 0.1°C 10-s detection). The knock-out mutants *myb21-2* and *myb21-3* generated via CRISPR/Cas9 were characterized by sequencing (Eurofins) the purified 500 bp PCR product flanking the single guide RNA target sites in the second exon of *SlMYB21*. In comparison with the wild-type sequence, either a T- deletion or T-insertion was detected. To identify homozygous *myb21-2* plants in the complementation approach, the silent mutation at the beginning of the second exon within the transgene was checked additionally in the PCR product sequence (primer myb21-2_for and 8245_rev). All primer pairs are listed in Supplemental Table 8.

Statistical Analysis

One-way analysis of variance (one-way ANOVA) followed by Tukey Honestly Significant Difference Test for statistical significance was performed using the VassarStats website for Statistical Computation (VassarStats) or R (R Core Team; https://www.r-project.org/). Two group comparisons between wild type and mutant samples were done using the Student's *t* test. Means were considered significantly different based on threshold value corresponding to $P < 0.05$ (ANOVA) or $P < 0.05$, $P < 0.01$, and $P < 0.001$ as indicated by (*), (**) and (***), respectively, (Student's *t* test). Detailed results of tests are shown in Supplemental Data Set 3.

Accession Numbers

The original Agilent GeneChip data as well as normalized data from this study are publicly available at ArrayExpress database (http://www.ebi.ac.uk/arrayexpress/) under accession number E-MTAB-7544. Sequence data (FASTQ files from RNA-seq experiments) from this article can be found at in the ArrayExpress database under accession number E-MTAB-7545.

Sequence data from key genes in this article can be found in the GenBank/EMBL/Solgenomics databases under the following accession numbers: *SlMYB21, Solyc02g067760; SlJAZ1, Solyc07g042170; SlJAZ2, Solyc12g009220; SlJAZ3, Solyc03g122190; SlJAZ4, Solyc12g049400; SlJAZ5, Solyc03g118540, SlJAZ6, Solyc01g005440; SlJAZ7, Solyc11g011030; SlJAZ8, Solyc06g068930; SlJAZ9, Solyc08g036640; SlJAZ10, Solyc08g036620; SlJAZ11, Solyc08g036660; SlJAZ13, Solyc01g103600; SlCOI1, Solyc05g052620; AtMYB21, At3g27810.*

Supplemental Data

Supplemental Figure 1. Carpels of *jai1-1* show enhanced growth in comparison to wild type.

Supplemental Figure 2. Morphology of wild type and *jai1-1* ovules (stages 1 – 4).

Supplemental Figure 3. *SlMYB21* encodes a flower specific MYB domain protein.

Supplemental Figure 4. splitTALE assay testing the interaction of SlMYB21 with JAZ9 fused to activation and binding domain of TALE, respectively.

Supplemental Figure 5. TILLING line *Slmyb21-1* flowers and fruits show a phenotype similar to *jai1-1*.

Supplemental Figure 6. Wild type and *Slmyb21-2* flower buds at stage 3 differ in length and carpel weight.

Supplemental Figure 7. Gene ontology analysis of differentially regulated genes in carpels of *jai1-1* and *Slmyb21-2* in comparison to wild type.

Supplemental Table 1. Relative transcript levels in relation to *SlTIP41* of genes commonly down-regulated in *jai1-1* and *Slmyb21-2* as determined by RT-qPCR.

Supplemental Table 2. Relative transcript levels in relation to *SlTIP41* of genes commonly up-regulated in *jai1-1* and *Slmyb21-2* as determined by RT-qPCR.

Supplemental Table 3. Levels of gibberellins in carpels at stage 3 from wild type, *jai1-1* and *Slmyb21-2*.

Supplemental Table 4. Primer sequences for RT-qPCR.

Supplemental Table 5. Primer sequences used for gateway cloning of JAZs and MYB21-CDS.

Supplemental Table 6. Primer sequences used for golden gate cloning.

Supplemental Table 7. Primer sequences for generation of Arabidopsis transformation construct using gateway cloning.

Supplemental Table 8. Primer sequences used for genotyping of *jai1-1*, *myb21* TILLING lines, *Slmyb21-2* and *Atmyb21-5*.

Supplemental Table 9. Primer sequences used for TILLING.

Supplemental Data Set 1. Tomato genes found in the microarray data to be differentially regulated in ovules of wild type and *jai1-1* plants.

Supplemental Data Set 2. Tomato genes found in the RNA-seq data to be differentially regulated in carpels of wild type, *jai1-1* and *Slmyb21-2* plants.

Supplemental Data Set 3. Results of student's *t* tests and ANOVA of quantitative data.

ACKNOWLEDGMENTS

We thank Hagen Stellmach and Merve Kuru (IPB Halle) for help in JA and JA-Ile quantification, BiFC approaches, and qPCR. Simone Fraas (Martin-Luther-University Halle-Wittenberg) is acknowledged for performing sectioning of tomato carpels, and Gregg Howe (Michigan State University) and Jason Reed (University of North Carolina) for providing seeds of *Sljai1-1* and *Atmyb21-5*, respectively. We thank Edelgard Wendeler (MPIPZ Cologne) for technical support. Tomato seeds (TOMJPE7564, TOMJPE7979, TOMJPE8245, TOMJPW0469) were provided by University of Tsukuba, Gene Research Center, through the National Bio-Resource Project (NBRP) of the AMED. Claus Wasternack (IPB Halle) is highly acknowledged for critical reading of the manuscript. This work was supported by Deutsche Forschungsgemeinschaft (DFG) (grant HA2655/12-1), the Czech Science Foundation (Grantová agentura České republiky) (grant 18-10349S), and the European Regional Developmental Fund Project "Centre for Experimental Plant Biology" (grant CZ.02.1.01/0.0/0.0/16_019/0000738).

AUTHOR CONTRIBUTIONS

R.S., S.D., S.M., and B.H. designed the research; R.S., S.D., C.G., G.H., T.S., Y.O., H.E., I.F.A., and D.T. performed research; R.S., S.D., B.A., D.T., and B.H. analyzed data; and R.S. and B.H. wrote the article with input from all authors.

Received January 2, 2019; revised February 19, 2019; accepted March 19, 2019; published March 20, 2019.

REFERENCES

Balcke, G.U., Handrick, V., Bergau, N., Fichtner, M., Henning, A., Stellmach, H., Tissier, A., Hause, B., and Frolov, A. (2012). An UPLC-MS/MS method for highly sensitive high-throughput analysis of phytohormones in plant tissues. Plant Methods **8:** 47.

Bradford, K.J., and Trewavas, A.J. (1994). Sensitivity thresholds and variable time scales in plant hormone action. Plant Physiol. **105:** 1029–1036.

Brooks, C., Nekrasov, V., Lippman, Z.B., and Van Eck, J. (2014). Efficient gene editing in tomato in the first generation using the clustered regularly interspaced short palindromic repeats/CRISPR-associated9 system. Plant Physiol. **166:** 1292–1297.

Browse, J. (2009a). The power of mutants for investigating jasmonate biosynthesis and signaling. Phytochemistry **70:** 1539–1546.

Browse, J. (2009b). Jasmonate passes muster: A receptor and targets for the defense hormone. Annu. Rev. Plant Biol. **60:** 183–205.

Brukhin, V., Hernould, M., Gonzalez, N., Chevalier, C., and Mouras, A. (2003). Flower development schedule in tomato *Lycopersicon esculentum* cv. sweet cherry. Sex. Plant Reprod. **15:** 311–320.

Carrera, E., Ruiz-Rivero, O., Peres, L.E.P., Atares, A., and Garcia-Martinez, J.L. (2012). Characterization of the *procera* tomato mutant shows novel functions of the SlDELLA protein in the control of flower morphology, cell division and expansion, and the auxin-signaling pathway during fruit-set and development. Plant Physiol. **160:** 1581–1596.

Čermák, T., Baltes, N.J., Čegan, R., Zhang, Y., and Voytas, D.F. (2015). High-frequency, precise modification of the tomato genome. Genome Biol. **16:** 232.

Chini, A., Fonseca, S., Fernández, G., Adie, B., Chico, J.M., Lorenzo, O., García-Casado, G., López-Vidriero, I., Lozano, F.M., Ponce, M.R., Micol, J.L., and Solano, R. (2007). The JAZ family of repressors is the missing link in jasmonate signalling. Nature **448:** 666–671.

Clough, S.J., and Bent, A.F. (1998). Floral dip: A simplified method for *Agrobacterium*-mediated transformation of *Arabidopsis thaliana.* Plant J. **16:** 735–743.

de Jong, M., Wolters-Arts, M., Feron, R., Mariani, C., and Vriezen, W.H. (2009). The *Solanum lycopersicum* auxin response factor 7 (SlARF7) regulates auxin signaling during tomato fruit set and development. Plant J. **57:** 160–170.

de Jong, M., Wolters-Arts, M., Schimmel, B.C.J., Stultiens, C.L.M., de Groot, P.F.M., Powers, S.J., Tikunov, Y.M., Bovy, A.G., Mariani, C., Vriezen, W.H., and Rieu, I. (2015). *Solanum lycopersicum* AUXIN RESPONSE FACTOR 9 regulates cell division activity during early tomato fruit development. J. Exp. Bot. **66:** 3405–3416.

Dobritzsch, S., Weyhe, M., Schubert, R., Dindas, J., Hause, G., Kopka, J., and Hause, B. (2015). Dissection of jasmonate functions in tomato stamen development by transcriptome and metabolome analyses. BMC Biol. **13:** 28.

Drews, G.N., and Yadegari, R. (2002). Development and function of the angiosperm female gametophyte. Annu. Rev. Genet. **36:** 99–124.

Eck, J.V., Kirk, D.D., and Walmsley, A.M. (2006). Tomato (*Lycopersicum esculentum*). In Agrobacterium Protocols, K. Wang, ed (Totowa, NJ: Humana Press), pp. 459–474.

Endress, P.K. (2010). Flower structure and trends of evolution in eudicots and their major subclades. Ann. Mo. Bot. Gard. **97:** 541–583.

Endress, P.K. (2011). Angiosperm ovules: Diversity, development, evolution. Ann. Bot. **107:** 1465–1489.

Engler, C., Youles, M., Gruetzner, R., Ehnert, T.-M., Werner, S., Jones, J.D.G., Patron, N.J., and Marillonnet, S. (2014). A golden gate modular cloning toolbox for plants. ACS Synth. Biol. **3:** 839–843.

Expósito-Rodríguez, M., Borges, A.A., Borges-Pérez, A., and Pérez, J.A. (2008). Selection of internal control genes for quantitative real-time RT-PCR studies during tomato development process. BMC Plant Biol. **8:** 131.

Fernandez, A.I., et al. (2009). Flexible tools for gene expression and silencing in tomato. Plant Physiol. **151:** 1729–1740.

Fonseca, S., Chini, A., Hamberg, M., Adie, B., Porzel, A., Kramell, R., Miersch, O., Wasternack, C., and Solano, R. (2009). (+)-7-*iso*-Jasmonoyl-L-isoleucine is the endogenous bioactive jasmonate. Nat. Chem. Biol. **5:** 344–350.

García-Hurtado, N., Carrera, E., Ruiz-Rivero, O., López-Gresa, M.P., Hedden, P., Gong, F., and García-Martínez, J.L. (2012). The characterization of transgenic tomato overexpressing *gibberellin 20-oxidase* reveals induction of parthenocarpic fruit growth, higher yield, and alteration of the gibberellin biosynthetic pathway. J. Exp. Bot. **63:** 5803–5813.

Gietz, R.D., and Schiestl, R.H. (2007). Large-scale high-efficiency yeast transformation using the LiAc/SS carrier DNA/PEG method. Nat. Protoc. **2:** 38–41.

Gillaspy, G., Ben-David, H., and Gruissem, W. (1993). Fruits: A developmental perspective. Plant Cell **5:** 1439–1451.

Goetz, S., Hellwege, A., Stenzel, I., Kutter, C., Hauptmann, V., Forner, S., McCaig, B., Hause, G., Miersch, O., Wasternack, C., and Hause, B. (2012). Role of *cis*-12-oxo-phytodienoic acid in tomato embryo development. Plant Physiol. **158:** 1715–1727.

Goldental-Cohen, S., Israeli, A., Ori, N., and Yasuor, H. (2017). Auxin response dynamics during wild-type and *entire* flower development in tomato. Plant Cell Physiol. **58:** 1661–1672.

Gorguet, B., van Heusden, A.W., and Lindhout, P. (2005). Parthenocarpic fruit development in tomato. Plant Biol (Stuttg) **7:** 131–139.

Grefen, C., and Blatt, M.R. (2012). A 2in1 cloning system enables ratiometric bimolecular fluorescence complementation (rBiFC). Biotechniques **53:** 311–314.

Haughn, G., and Chaudhury, A. (2005). Genetic analysis of seed coat development in Arabidopsis. Trends Plant Sci. **10:** 472–477.

Hause, B., Stenzel, I., Miersch, O., Maucher, H., Kramell, R., Ziegler, J., and Wasternack, C. (2000). Tissue-specific oxylipin signature of tomato flowers: Allene oxide cyclase is highly expressed in distinct flower organs and vascular bundles. Plant J. **24:** 113–126.

Hedden, P., and Phillips, A.L. (2000). Manipulation of hormone biosynthetic genes in transgenic plants. Curr. Opin. Biotechnol. **11:** 130–137.

Hedden, P., and Thomas, S.G. (2012). Gibberellin biosynthesis and its regulation. Biochem. J. **444:** 11–25.

Hu, J., Israeli, A., Ori, N., and Sun, T.P. (2018). The interaction between DELLA and ARF/IAA mediates crosstalk between gibberellin and auxin signaling to control fruit initiation in tomato. Plant Cell **30:** 1710–1728.

Huang, H., Gao, H., Liu, B., Qi, T., Tong, J., Xiao, L., Xie, D., and Song, S. (2017). *Arabidopsis MYB24* regulates jasmonate-mediated stamen development. Front. Plant Sci. **8:** 1525.

Johri, B., Ambegaokar, K., and Srivastava, P. (1992). Comparative embryology of angiosperms. (Berlin: Springer).

Kapil, R., and Tiwari, S. (1978). The integumentary tapetum. Bot. Rev. **44:** 457–490.

Kay, S., Hahn, S., Marois, E., Hause, G., and Bonas, U. (2007). A bacterial effector acts as a plant transcription factor and induces a cell size regulator. Science **318:** 648–651.

Larsson, E., Roberts, C.J., Claes, A.R., Franks, R.G., and Sundberg, E. (2014). Polar auxin transport is essential for medial versus lateral tissue specification and vascular-mediated valve outgrowth in Arabidopsis gynoecia. Plant Physiol. **166:** 1998–2012.

Li, L., Zhao, Y., McCaig, B.C., Wingerd, B.A., Wang, J., Whalon, M.E., Pichersky, E., and Howe, G.A. (2004). The tomato homolog of CORONATINE-INSENSITIVE1 is required for the maternal control of seed maturation, jasmonate-signaled defense responses, and glandular trichome development. Plant Cell **16:** 126–143.

Liu, Z., Miao, L., Huo, R., Song, X., Johnson, C., Kong, L., Sundaresan, V., and Yu, X. (2018). ARF2–ARF4 and ARF5 are essential for female and male gametophyte development in Arabidopsis. Plant Cell Physiol. **59:** 179–189.

Lu, J., and Magnani, E. (2018). Seed tissue and nutrient partitioning, a case for the nucellus. Plant Reprod. **31:** 309–317

Machemer, K., Shaiman, O., Salts, Y., Shabtai, S., Sobolev, I., Belausov, E., Grotewold, E., and Barg, R. (2011). Interplay of MYB factors in differential cell expansion, and consequences for tomato fruit development. Plant J. **68:** 337–350.

Mandaokar, A., and Browse, J. (2009). MYB108 acts together with MYB24 to regulate jasmonate-mediated stamen maturation in Arabidopsis. Plant Physiol. **149:** 851–862.

Mandaokar, A., Thines, B., Shin, B., Lange, B.M., Choi, G., Koo, Y.J., Yoo, Y.J., Choi, Y.D., Choi, G., and Browse, J. (2006). Transcriptional regulators of stamen development in *Arabidopsis* identified by transcriptional profiling. Plant J. **46:** 984–1008.

Marsch-Martínez, N., and de Folter, S. (2016). Hormonal control of the development of the gynoecium. Curr. Opin. Plant Biol. **29:** 104–114.

Merico, D., Isserlin, R., Stueker, O., Emili, A., and Bader, G.D. (2010). Enrichment map: A network-based method for gene-set enrichment visualization and interpretation. PLoS One **5:** e13984.

Meyer, Y., Grosset, J., Chartier, Y., and Cleyet-Marel, J.-C. (1988). Preparation by two-dimensional electrophoresis of proteins for antibody production: antibodies against proteins whose synthesis is reduced by auxin in tobacco mesophyll protoplasts. Electrophoresis **9:** 704–712.

Mielke, K., Forner, S., Kramell, R., Conrad, U., and Hause, B. (2011). Cell-specific visualization of jasmonates in wounded tomato and *Arabidopsis* leaves using jasmonate-specific antibodies. New Phytol. **190:** 1069–1080.

Modrusan, Z., Reiser, L., Feldmann, K.A., Fischer, R.L., and Haughn, G.W. (1994). Homeotic transformation of ovules into carpel-like structures in Arabidopsis. Plant Cell **6:** 333–349.

Moubayidin, L., and Østergaard, L. (2017). Gynoecium formation: An intimate and complicated relationship. Curr. Opin. Genet. Dev. **45:** 15–21.

Nekrasov, V., Staskawicz, B., Weigel, D., Jones, J.D.G., and Kamoun, S. (2013). Targeted mutagenesis in the model plant *Nicotiana benthamiana* using Cas9 RNA-guided endonuclease. Nat. Biotechnol. **31:** 691–693.

Niwa, T., Suzuki, T., Takebayashi, Y., Ishiguro, R., Higashiyama, T., Sakakibara, H., and Ishiguro, S. (2018). Jasmonic acid facilitates flower opening and floral organ development through the upregulated expression of SlMYB21 transcription factor in tomato. Biosci. Biotechnol. Biochem. **82:** 292–303.

Okabe, Y., Asamizu, E., Saito, T., Matsukura, C., Ariizumi, T., Brès, C., Rothan, C., Mizoguchi, T., and Ezura, H. (2011). Tomato TILLING technology: Development of a reverse genetics tool for the efficient isolation of mutants from Micro-Tom mutant libraries. Plant Cell Physiol. **52:** 1994–2005.

Pattison, R.J., Csukasi, F., and Catalá, C. (2014). Mechanisms regulating auxin action during fruit development. Physiol. Plant. **151:** 62–72.

Qi, T., Huang, H., Song, S., and Xie, D. (2015). Regulation of jasmonate-mediated stamen development and seed production by a bHLH-MYB complex in Arabidopsis. Plant Cell **27:** 1620–1633.

Reeves, P.H., et al. (2012). A regulatory network for coordinated flower maturation. PLoS Genet. **8:** e1002506.

Rittenberg, D., and Foster, G.L. (1940). A new procedure for quantitative analysis by isotope dilution with application to the determination of amino acids and fatty acids. J. Biol. Chem. **133:** 737–744.

Schmittgen, T.D., and Livak, K.J. (2008). Analyzing real-time PCR data by the comparative C(T) method. Nat. Protoc. **3:** 1101–1108.

Schneitz, K., Hülskamp, M., and Pruitt, R.E. (1995). Wild-type ovule development in *Arabidopsis thaliana*: A light microscope study of cleared whole-mount tissue. Plant J. **7:** 731–749.

Schreiber, T., and Tissier, A. (2016). Libraries of synthetic TALE-activated promoters: Methods and applications. In Meth. Enzymol., S.E. O'Connor, ed (London: Academic Press), pp. 361–378.

Schreiber, T., Prange, A., Hoppe, T., and Tissier, A.F. (2019). Split-TALE: A TALE-based two-component system for synthetic biology applications in planta. Plant Physiol **179:**1001–1012.

Serrani, J., Fos, M., Atarés, A., and García-Martínez, J. (2007). Effect of gibberellin and auxin on parthenocarpic fruit growth induction in the cv Micro-Tom of tomato. J. Plant Growth Regul. **26:** 211–221.

Shimada, T.L., Shimada, T., and Hara-Nishimura, I. (2010). A rapid and non-destructive screenable marker, FAST, for identifying transformed seeds of *Arabidopsis thaliana.* Plant J. **61:** 519–528.

Smyth, D.R., Bowman, J.L., and Meyerowitz, E.M. (1990). Early flower development in Arabidopsis. Plant Cell **2:** 755–767.

Song, S., Qi, T., Huang, H., Ren, Q., Wu, D., Chang, C., Peng, W., Liu, Y., Peng, J., and Xie, D. (2011). The Jasmonate-ZIM domain proteins interact with the R2R3-MYB transcription factors MYB21 and MYB24 to affect Jasmonate-regulated stamen development in Arabidopsis. Plant Cell **23:** 1000–1013.

Sparkes, I.A., Runions, J., Kearns, A., and Hawes, C. (2006). Rapid, transient expression of fluorescent fusion proteins in tobacco plants and generation of stably transformed plants. Nat. Protoc. **1:** 2019–2025.

Spurr, A.R. (1969). A low-viscosity epoxy resin embedding medium for electron microscopy. J. Ultrastruct. Res. **26:** 31–43.

Subramanian, A., Tamayo, P., Mootha, V.K., Mukherjee, S., Ebert, B.L., Gillette, M.A., Paulovich, A., Pomeroy, S.L., Golub, T.R., Lander, E.S., and Mesirov, J.P. (2005). Gene set enrichment analysis: A knowledge-based approach for interpreting genome-wide expression profiles. Proc. Natl. Acad. Sci. USA **102:** 15545–15550.

Thines, B., Katsir, L., Melotto, M., Niu, Y., Mandaokar, A., Liu, G., Nomura, K., He, S.Y., Howe, G.A., and Browse, J. (2007). JAZ repressor proteins are targets of the SCF(^{COI1}) complex during jasmonate signalling. Nature **448:** 661–665.

Urbanová, T., Tarkowská, D., Novák, O., Hedden, P., and Strnad, M. (2013). Analysis of gibberellins as free acids by ultra performance liquid chromatography-tandem mass spectrometry. Talanta **112:** 85–94.

Varaud, E., Brioudes, F., Szécsi, J., Leroux, J., Brown, S., Perrot-Rechenmann, C., and Bendahmane, M. (2011). AUXIN RESPONSE FACTOR8 regulates *Arabidopsis* petal growth by interacting with the bHLH transcription factor BIGPETALp. Plant Cell **23:** 973–983.

Wang, H., Schauer, N., Usadel, B., Frasse, P., Zouine, M., Hernould, M., Latché, A., Pech, J.-C., Fernie, A.R., and Bouzayen, M. (2009). Regulatory features underlying pollination-dependent and -independent tomato fruit set revealed by transcript and primary metabolite profiling. Plant Cell **21:** 1428–1452.

Wasternack, C., and Hause, B. (2013). Jasmonates: Biosynthesis, perception, signal transduction and action in plant stress response, growth and development. An update to the 2007 review in Annals of Botany. Ann. Bot. **111:** 1021–1058.

Wasternack, C., and Song, S. (2017). Jasmonates: Biosynthesis, metabolism, and signaling by proteins activating and repressing transcription. J. Exp. Bot. **68:** 1303–1321.

Weber, E., Engler, C., Gruetzner, R., Werner, S., and Marillonnet, S. (2011). A modular cloning system for standardized assembly of multigene constructs. PLoS One **6:** e16765.

Werner, S., Engler, C., Weber, E., Gruetzner, R., and Marillonnet, S. (2012). Fast track assembly of multigene constructs using Golden Gate cloning and the MoClo system. Bioeng. Bugs **3:** 38–43.

Xu, W., Fiume, E., Coen, O., Pechoux, C., Lepiniec, L., and Magnani, E. (2016). Endosperm and nucellus develop antagonistically in Arabidopsis seeds. Plant Cell **28:** 1343–1360.

Yoo, S.-D., Cho, Y.-H., and Sheen, J. (2007). Arabidopsis mesophyll protoplasts: A versatile cell system for transient gene expression analysis. Nat. Protoc. **2:** 1565–1572.

Zouine, M., Maza, E., Djari, A., Lauvernier, M., Frasse, P., Smouni, A., Pirrello, J., and Bouzayen, M. (2017). TomExpress, a unified tomato RNA-Seq platform for visualization of expression data, clustering and correlation networks. Plant J. **92:** 727–735.